

# Accepted Manuscript

Increasing the Binding Affinity of VEGFR-2 Inhibitors by Extending their Hydrophobic Interaction with the Active Site: Design, Synthesis and Biological Evaluation of 1-Substituted-4-(4-methoxybenzyl)phthalazine Derivatives

Wagdy M. Eldehna, Sahar M. Abou-Seri, Ahmed M. El Kerdawy, Rezk R. Ayyad, Abdallah M. Hamdy, Hazem A. Ghabbour, Mamdouh M. Ali, Dalal A. Abou El Ella

PII: S0223-5234(16)30109-X

DOI: [10.1016/j.ejmech.2016.02.029](https://doi.org/10.1016/j.ejmech.2016.02.029)

Reference: EJMECH 8380

To appear in: *European Journal of Medicinal Chemistry*

Received Date: 24 November 2015

Revised Date: 9 February 2016

Accepted Date: 10 February 2016

Please cite this article as: W.M. Eldehna, S.M. Abou-Seri, A.M. El Kerdawy, R.R. Ayyad, A.M. Hamdy, H.A. Ghabbour, M.M. Ali, D.A. Abou El Ella, Increasing the Binding Affinity of VEGFR-2 Inhibitors by Extending their Hydrophobic Interaction with the Active Site: Design, Synthesis and Biological Evaluation of 1-Substituted-4-(4-methoxybenzyl)phthalazine Derivatives, *European Journal of Medicinal Chemistry* (2016), doi: 10.1016/j.ejmech.2016.02.029.

This is a PDF file of an unedited manuscript that has been accepted for publication. As a service to our customers we are providing this early version of the manuscript. The manuscript will undergo copyediting, typesetting, and review of the resulting proof before it is published in its final form. Please note that during the production process errors may be discovered which could affect the content, and all legal disclaimers that apply to the journal pertain.

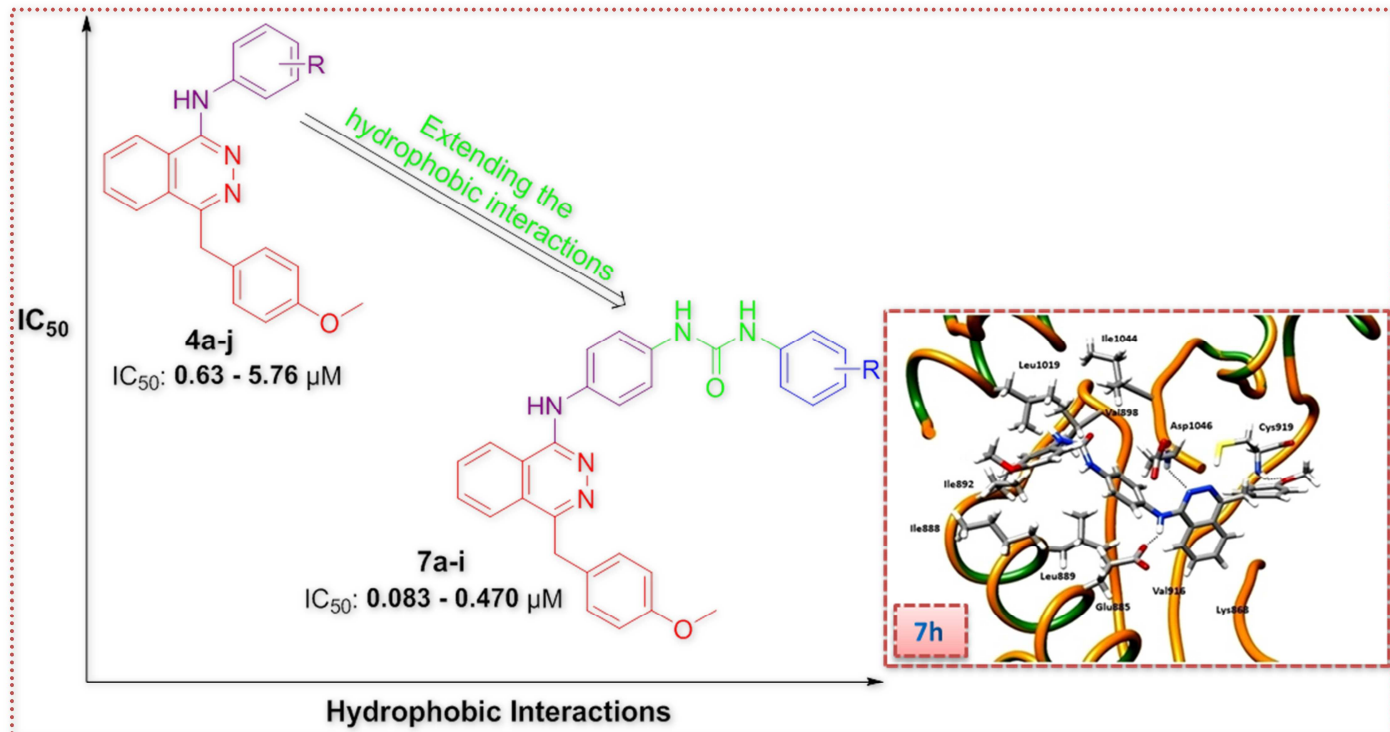


## Graphical abstract

### **Increasing VEGFR-2 Inhibitors Binding Affinity by Extending their Hydrophobic Interaction with the Active Site: Design, Synthesis and Biological Evaluation of 4-(4-Methoxybenzyl)phthalazine Derivatives as Novel VEGFR-2 Inhibitors**

Wagdy M. Eldehna\*, Sahar M. Abou-Seri\*, Ahmed M. El Kerdawy, Rezk R. Ayyad, Hazem A. Ghabbour, Mamdouh M. Ali, Dalal A. Abou El Ella

Extending the anilinophthalazine derivatives **4** with a substituted phenyl moiety through an uriedo linker increased the hydrophobic interaction of uriedo-anilinophthalazine derivatives **7** within the hydrophobic back pocket.



## Increasing the Binding Affinity of VEGFR-2 Inhibitors by Extending their Hydrophobic Interaction with the Active Site: Design, Synthesis and Biological Evaluation of 1-Substituted-4-(4-methoxybenzyl)phthalazine Derivatives

Wagdy M. Eldehna<sup>a,\*</sup>, Sahar M. Abou-Seri<sup>b,c,\*</sup>, Ahmed M. El Kerdawy<sup>b,c</sup>, Rezk R. Ayyad<sup>d,e</sup>, Abdallah M. Hamdy<sup>f</sup>, Hazem A. Ghabbour<sup>g</sup>, Mamdouh M. Ali<sup>h</sup>, Dalal A. Abou El Ella<sup>i</sup>

<sup>a</sup>Department of Pharmaceutical Chemistry, Faculty of Pharmacy, Egyptian Russian University, Badr City, Cairo, P.O. Box 11829, Egypt.

<sup>b</sup>Department of Pharmaceutical Chemistry, Faculty of Pharmacy, Cairo University, Kasr El-Aini Street, Cairo, P.O. Box 11562, Egypt.

<sup>c</sup>Molecular Modeling Unit, Faculty of Pharmacy, Cairo University, Kasr El-Aini Street, Cairo, P.O. Box 11562, Egypt.

<sup>d</sup>Department of Pharmaceutical Chemistry, Faculty of Pharmacy, Al-Azhar University, Cairo, Egypt.

<sup>e</sup>Department of Pharmaceutical Chemistry, Faculty of Pharmacy, Delta University For Science and Technology, Mansoura, Egypt.

<sup>f</sup>Department of Analytical Chemistry, Faculty of Pharmacy, Egyptian Russian University, Badr City, Cairo, P.O. Box 11829, Egypt.

<sup>g</sup>Department of Pharmaceutical Chemistry, College of Pharmacy, King Saud University, P.O. Box 2457, Riyadh 11451, Saudi Arabia.

<sup>h</sup>Biochemistry Department, Division of Genetic Engineering and Biotechnology, National Research Centre, Dokki 12622, Giza, Egypt.

<sup>i</sup>Department of Pharmaceutical Chemistry, Faculty of Pharmacy, Ain Shams University, Cairo, Abbassia, P.O. Box 11566, Egypt.

### Abstract

A series of anilinophthalazine derivatives **4a-j** was initially synthesized and tested for its VEGFR-2 inhibitory activity where it showed promising activity ( $IC_{50}=0.636-5.76 \mu M$ ). Molecular docking studies guidance was used to improve the binding affinity for series **4a-j** towards VEGFR-2 active site. This improvement was achieved by increasing the hydrophobic interaction with the hydrophobic back pocket of the VEGFR-2 active site lined with the hydrophobic side chains of Ile888, Leu889, Ile892, Val898, Val899, Leu1019 and Ile1044. Increasing the hydrophobic interaction was accomplished by extending the anilinophthalazine scaffold with a substituted phenyl moiety through an uriedo linker which should give this extension the flexibility required to accommodate itself deeply into the hydrophobic back pocket. As planned, the designed uriedo-anilinophthalazines **7a-i** showed superior binding affinity than their anilinophthalazine parents ( $IC_{50}=0.083-0.473 \mu M$ ). In particular,

compounds **7g-i** showed  $IC_{50}$  of 0.086, 0.083 and 0.086  $\mu\text{M}$ , respectively, which are better than that of the reference drug sorafenib ( $IC_{50}=0.09 \mu\text{M}$ ).

*Keywords:* Phthalazine; VEGFR-2; hydrophobic interaction.

\*Corresponding author. Department of Pharmaceutical Chemistry, Faculty of Pharmacy, Egyptian Russian University, Cairo, Egypt. [wagdy2000@gmail.com](mailto:wagdy2000@gmail.com) (W.M. Eldehna),

\*Corresponding author. Department of Pharmaceutical Chemistry, Faculty of Pharmacy, Cairo University, Cairo, Egypt. [saharshaarawy\\_69@yahoo.com](mailto:saharshaarawy_69@yahoo.com) (S.M. Abou-Seri).

## 1. Introduction

Angiogenesis, the process of new blood vessel growth from the quiescent pre-existing vessels, is a critical and complex process in both physiological and pathophysiological conditions [1]. The process is regulated by a balance between pro- and antiangiogenic molecules, and is derailed in various diseases, especially cancer [2]. In 1971, Folkman [3] proposed that tumor growth and metastasis are angiogenesis-dependent, and hence, blocking angiogenesis could be a strategy to hinder tumor growth.

Among the various players at the molecular level involved in the different mechanisms of vascular growth, members of the vascular endothelial growth factor (VEGF) family have a predominant role [4]. Vascular endothelial growth factor (VEGF) represents a family of homodimeric glycoproteins which are critical for vasculogenesis, lymphangiogenesis and angiogenesis [5]. VEGF ligands bind in an overlapping pattern to three different, but structurally related, VEGF-receptor tyrosine kinases (VEGFR-TK) which are VEGFR-1 (Flt-1), VEGFR-2 (KDR) and VEGFR-3 (Flt-4) [6].

VEGFR-2, a type III transmembrane tyrosine kinase receptor, is critical for angiogenesis [7]. Hence, VEGFR-2 inhibition emerged as a prime approach for discovering new therapies for many human angiogenesis-dependent malignancies. To date, a humanized anti-VEGF monoclonal antibody (bevacizumab) and several small molecule VEGFR-2 kinase inhibitors (sorafenib, regorafenib, sunitinib, vandetanib, pazopanib, axitinib and cabozantinib) have been approved as antiangiogenic drugs [8].

Phthalazine derivatives have attracted considerable attention as antitumor agents [9-14]. In this context, 1-anilino-4-aryl-phthalazine scaffold in particular emerged as an interesting scaffold for designing VEGFR inhibitors. The first published anilinophthalazine derivative as a potent VEGFR inhibitor was vatalanib (PTK787) **I** (Figure 1) [15]. Vatalanib **I** is one of the most potent and selective VEGFR kinase inhibitors, with  $IC_{50}$  value of 43 nM for VEGFR-2 [16]. Vatalanib **I** showed interesting results in many clinical trials on different tumor types, such as metastatic gastrointestinal stromal tumors (GIST), Non-small-cell lung carcinoma (NSCLC) and metastatic pancreatic cancer [17-19]. The disclosure of vatalanib as a clinical candidate paved the way for the design and synthesis of different anilinophthalazine derivatives as potent inhibitors for VEGFR-2 such as IM-023911 **II** with  $IC_{50} = 190$  nM (Figure 1) [20-24].

The aforementioned facts have motivated us to design novel 1-anilino-4-aryl-phthalazine derivatives with more potent VEGFR-2 inhibitory activity.

**Figure 1**

The essential pharmacophoric features in the anilinophthalazine VEGFR-2 inhibitors include (Figure 2): [23, 25]

a) Fused aromatic system represented by the phthalazine ring interacting as H-bond acceptor with its N2 with Asp1046 in the conserved DFG motif and through hydrophobic interaction with the side chains of Lys868 and Val916.

b) Substituted anilino moiety in position 1 of the phthalazine interacting as H-bond donor with its NH with the side chain carboxylate of Glu885 of the  $\alpha$ C helix and through hydrophobic interaction with its substituted phenyl moiety with the hydrophobic back pocket lined with the hydrophobic side chains of Ile888, Leu889, Ile892, Val898, Val899, Leu1019 and Ile1044.

c) Hydrogen bond acceptor represented by a lone pair of a nitrogen (as in vatalanib **I**) or oxygen atom (as in IM-023911 **II**) attached to position 4 of phthalazine via benzyl or phenyl moiety, which interacts with the backbone NH of Cys919 in the hinge region of the protein.

**Figure 2**

In the presented work, we introduce two series of anilinophthalazine derivatives [**4a-j** and **7a-i**] with different substitutions on the anilino moiety offering various electronic and lipophilic environments to study their impact on the activity (Figure 1). We also replaced the 4-pyridyl moiety in the vatalanib by the relatively longer 4-methoxyphenyl moiety which should make the oxygen lone pair more accessible for interaction with Cys919 NH group than that of the 4-pyridyl nitrogen.

Molecular docking studies were carried out to study the interaction of the newly synthesized compounds with VEGFR-2, their binding mode and their ability to satisfy the pharmacophoric features required to induce the desired inhibition. They were also used further as a guide to improve the binding between VEGFR-2 and the newly synthesized ligands.

The newly synthesized phthalazines **4a-j** and **7a-i** were evaluated for their potential VEGFR-2 inhibitory and anti-proliferative activities.

**2. Results and discussion***2.1. Chemistry*

The synthetic pathway employed to prepare the new phthalazine derivatives is outlined in Schemes 1-2. Synthesis was initiated by reacting phthalic anhydride with 4-methoxyphenylacetic acid in the presence of fused sodium acetate to afford 3-(4-methoxybenzylidene)isobenzofuran-1(3*H*)-one (**1**) [26], which was treated with hydrazine sulfate and sodium hydroxide to provide 4-(4-methoxybenzyl)phthalazin-1(2*H*)-one (**2**) [26]. The key intermediate 1-chloro-4-(4-methoxybenzyl)phthalazine (**3**) was prepared *via* chlorination of **2** with refluxing phosphorous oxychloride in the presence of a catalytic amount of *N,N*-dimethylaniline. The target compounds **4a-j** were obtained by coupling the chloro intermediate **3** with the appropriate aniline in a refluxing acetone (Scheme 1).

### Scheme 1

IR spectra of **4a-j** revealed the presence of an NH stretching band about 3300 cm<sup>-1</sup>. Their <sup>1</sup>H NMR spectra showed one D<sub>2</sub>O-exchangeable singlet signal attributed to the aniline NH proton in the region  $\delta$  9.41-11.16 *ppm*, while the benzylic CH<sub>2</sub> protons appeared as singlet signal in the region  $\delta$  4.43-4.74 *ppm*. Furthermore, the <sup>13</sup>C NMR spectra of compounds **4a-j** revealed the presence of the signal of the benzylic methylene carbon in the range  $\delta$  34.13-37.59 *ppm*, while the signal due to the carbon of the methoxy group appeared around 55 *ppm*.

For the synthesis of ureido derivatives **7a-i**, the 1-(4-aminophenyl)-3-phenylurea intermediates **6a-i** were synthesized by the reaction of 1-isocyanato-4-nitrobenzene with the adequate aniline to afford 1-(4-nitrophenyl)-3-phenylureas **5a-i** followed by hydrogenation using Pd/C [27]. The target diarylureas **7a-i** were prepared through the reaction of the key intermediate **3** and the corresponding 1-(4-aminophenyl)-3-phenylureas **6a-i** in a refluxing acetone (Scheme 2).

### Scheme 2

IR spectra of the latter products showed the absorption bands due to the (NH) and (C=O) groups in the regions  $\delta$  3244-3340 and 1666-1714 cm<sup>-1</sup>, respectively, whereas, their <sup>1</sup>H NMR spectra revealed the presence of three D<sub>2</sub>O-exchangeable singlet signals assigned to the two amidic NH groups and the secondary amino NH in the regions  $\delta$  8.57-10.16, 8.63-10.89 and 9.02-10.97 *ppm*, respectively. Besides, the <sup>13</sup>C NMR spectra of compounds **7a-i** showed three characteristic signals resonating in the range  $\delta$  158.04-158.13, 54.88-55.00 and 35.60-36.11 *ppm* attributable for the carbonyl, methoxy and benzylic methylene carbons, respectively.

## 2.2. Activity towards VEGFR-2 kinase

### 2.2.1. VEGFR-2 inhibitory assay

All newly synthesized compounds were evaluated *in vitro* for their VEGFR-2 inhibitory activity. Sorafenib **III** was included in the experiments as reference VEGFR-2 inhibitor. The results are reported as median inhibition concentrations ( $IC_{50}$ ) and summarized in Table 1.

As can be seen in Table 1, the novel phthalazine derivatives displayed moderate to potent VEGFR-2 inhibitory activity. Generally, series **7a-i** showed superior activity in comparison to series **4a-j** ( $IC_{50}$  = 0.083 - 0.473  $\mu$ M vs. 0.636 - 5.76  $\mu$ M, respectively). Among the tested phthalazine derivatives, compounds **7g-i** were found to be the most potent members with excellent VEGFR-2 inhibitory activity ( $IC_{50}$  = 0.086, 0.083 and 0.086  $\mu$ M, respectively) compared to sorafenib **III** ( $IC_{50}$  = 0.090  $\mu$ M). Compounds **4h**, **4j** and **7a-f** exhibited high potency at the sub-micromolar level with  $IC_{50}$  ranged from 0.114 to 0.754  $\mu$ M. On the other hand, compounds **4a-g** and **4i** were the least potent analogs with  $IC_{50}$  range of 1.34 - 5.76  $\mu$ M.

**Table 1**

### 2.2.2. Molecular docking study and structure activity relationship SAR

We started this work by the synthesis of a series of anilino-phthalazine derivatives with various substitutions on the anilino moiety **4a-j** to investigate the impact of this variable on activity. This series showed promising activity in the VEGFR-2 kinase inhibition assay with  $IC_{50}$  ranged between 0.636 and 5.76  $\mu$ M. At this stage molecular docking study was carried out to investigate their plausible binding pattern and their interaction with the key amino acids in the active site of the VEGFR-2. Information gained from the docking result analysis for compounds **4a-j** was used as a guide to perform some educated manipulations in their chemical structure to improve the series activity.

Several crystal structures are available in the protein data bank for VEGFR-2 [28], for this work we chose (PDB ID: 4ASD) [29] which has VEGFR-2 in the inactive conformation (DFG-out) co-crystallized with sorafenib as inhibitor.

First, the molecular docking protocol was validated by re-docking of the sorafenib ligand in the vicinity of the VEGFR-2 receptor active site. The re-docking validation step reproduced the experimental binding mode of the co-crystallized ligand quite efficiently indicating the suitability of the used setup for the intended docking study as demonstrated by the small

RMSD of 0.470 Å between the docked pose and the co-crystallized ligand (energy score (S) = -15.19 kcal/mol) and by the ability of the docking pose to reproduce all the key interactions accomplished by the co-crystallized ligand with the key amino acids in the active site (Glu885, Cys919 and Asp1046) (Figure 3)

### **Figure 3**

The ability of the synthesized compounds **4a-j** to interact with the key amino acids in the active site rationalizes their good activity as indicated by their docking pattern and docking score compared to that of sorafenib (Figure 4 and 5, Table 2). As can be seen in Figure 4, compound **4g** (as a representative for series **4a-j**) interacts by its phthalazine ring N2 through H-bond with Asp1046 of the conserved DFG motif exposing its benzene ring to the hydrophobic side chains of Lys868 and Val916. As H-bond donor, it interacts with its anilino NH with the side chain carboxylate of Glu885 of the  $\alpha$ C helix fitting its substituted phenyl moiety into the hydrophobic back pocket lined with the hydrophobic side chains of Ile888, Leu889, Ile892, Val898, Val899, Leu1019 and Ile1044. As planned the oxygen lone pair of the 4-methoxyphenyl moiety interacts as H-bond acceptor with the Cys919 NH group (2D diagrams and 3D representations for the rest of the series can be found in the supporting information).

### **Figure 4**

As indicated by the experimental assay (Tables 1) and supported by the docking energy score (Tables 2), the derivative with an unsubstituted anilino moiety **4a** has the lowest activity 5.76±0.58  $\mu$ M and docking energy score -14.74 kcal/mol. Addition of a hydrophobic substituent on the anilino moiety (**4b,4d-4i**) increases the binding affinity as indicated by their lower IC<sub>50</sub> (0.754±0.07 - 3.97±0.43  $\mu$ M) and better docking energy score (-15.06 - -16.32 kcal/mol) than the unsubstituted derivative **4a** which could be attributed to their increased hydrophobic interaction with the hydrophobic back pocket (left side of the Figure 4b). The superior activity of compound **4j** (IC<sub>50</sub> = 0.636±0.06  $\mu$ M) which is supported by its high docking score (-15.94 kcal/mol) can be attributed to the exposure of its hydrophilic sulphonamido moiety to the bulk solvent and its involvement in H-bonding with the imidazole ring of His1026 in the catalytic loop (Figure 5).

**Table 2****Figure 5**

Based on the docking results of the anilinophthalazine derivatives **4a-j**, another series **7a-i** was designed in an attempt to increase the binding affinity to VEGFR-2 active site through increasing the hydrophobic interaction with the hydrophobic back pocket. In this new series **7a-i**, series **4a-j** was extended with a second substituted phenyl group on the anilino moiety through an ureido linker (Figure 1) giving this second phenyl group the flexibility required to accommodate itself into the hydrophobic back pocket. The selection of the ureido linker is due to the reported anti-tumor activity of a vast array of urea containing compounds [30].

As planned, series **7a-i** showed better docking energy scores (*S*) compared to series **4a-j** (−17.85 to −20.25 kcal/mol vs. −14.74 to −16.32 kcal/mol, respectively) (Table 2) due to extension of the hydrophobic interaction with the hydrophobic back pocket. This hypothesis is augmented by the fact that increasing the hydrophobicity of the substituent(s) on the pendant phenyl ring increases the docking energy score (Table 2). In agreement with the docking energy scores (*S*), the expected superiority of series **7a-i** was experimentally proven by their lower IC<sub>50</sub> values in comparison to series **4a-j** (Table 1). Figure 6 shows the proposed binding mode of series **7a-i** as represented by compound **7h** docking pose in the VEGFR-2 active site indicating that series **7a-i** does not only fulfill the key interactions required for VEGFR-2 inhibition with the key amino acids in the active site (Glu885, Cys919 and Asp1046) as series **4a-j** does (figure 4) but also extending with their phenyl ureido moiety into the hydrophobic back pocket achieving additional hydrophobic interaction which is responsible for their higher docking score and consequently higher VEGFR-2 inhibitory activity than that of series **4a-j** (table 1 and table 2)

**Figure 6*****2.3. In vitro anti-proliferative activity.***

All the newly synthesized compounds were selected by the National Cancer Institute (NCI) Developmental Therapeutic Program ([www.dtp.nci.nih.gov](http://www.dtp.nci.nih.gov)) to be screened for their anticancer activity *in vitro*. The anticancer assays were performed in accordance with the protocol of the Drug Evaluation Branch, NCI, Bethesda [31-33].

The compounds were evaluated at one dose primary anticancer assay towards a panel of approximately 60 cancer cell lines (concentration  $10^{-5}$  M). The human tumor cell lines were taken from nine different organs (blood, skin, lung, colon, brain, ovary, kidney, prostate and breast). A 48 h drug exposure protocol was used and sulforhodamine B (SRB) protein assay was applied to estimate the cell viability and growth [34]. The data reported as mean-graph of the percent growth of the treated cells, and presented as percentage growth inhibition (GI%) caused by the test compounds (Table 3).

The tested compounds displayed different levels of anticancer activity and possessed a distinctive pattern of selectivity against the tested cancer cell lines.

Close examination of the GI% values in Table 3, revealed that compounds **4b**, **4e-g**, **7c**, **7f**, **7g** and **7i** are the most active analogues in this study, showing broad spectrum activity toward numerous cell lines that belong to different tumor subpanels. In particular, compound **4g** emerged as the most active member with mean inhibition = 44 %. It possessed antiproliferative activity against 44 cell lines representing all subpanels (GI; 32-94 %) with potent growth inhibitory effect over leukemia MOLT-4 and RPMI-8226, non-small cell lung cancer NCI-H460, colon cancer HCT-116, renal cancer UO-31 and prostate cancer PC-3 with inhibition % 69, 94, 74, 73, 63 and 61, respectively. On the contrary, compounds **4d** and **4j** have not shown any significant cytotoxic activity against any cell line. Nevertheless, compounds **4a**, **4c**, **7d** and **7h** possessed fair and selective growth inhibitory activity against sporadic cell lines.

### Table 3

Regarding sensitivity of individual cell lines (Figure 7), leukemia RPMI-8226 was the most susceptible cell line to the majority of compounds, especially compounds **4b**, **4e**, **4g**, **4h**, **7c** and **7i** displayed strong antiproliferative activity with GI % > 80. Meanwhile, compound **7i** showed potent growth inhibition against renal cancer RXF 393 and breast cancer HS 578T (GI %= 100 and 96, respectively). Moreover, compounds **7c** and **7f** exerted cytotoxic effect with GI more than 100% against certain cell lines. Compound **7c** was proved to be lethal to renal cancer RXF 393 and breast cancer HS 578T cell lines (GI %= 110 and 105, respectively), while **7f** exerted lethal activity over non-small cell lung cancer NCI-H460 with GI %=110.

A control experiment was carried out to rule out that the compounds' low cytotoxic activity is due to the binding interaction between the hydrophobic tested compounds and the serum albumin used in the experiment. [For further details, see Supporting Information]

### 3. Conclusion

The newly synthesized anilinophthalazine derivatives **4a-j** showed promising activity in the VEGFR-2 kinase inhibition assay with  $IC_{50}$  ranged between 0.636 and 5.76  $\mu\text{M}$ . Molecular docking studies guided their binding affinity improvement through increasing the hydrophobic interaction of the synthesized inhibitors with the hydrophobic back pocket of the VEGFR-2 active site. Extending the anilinophthalazine scaffold with a substituted phenyl moiety through an uriedo linker was the used strategy to increase the hydrophobic interaction with the hydrophobic back pocket. The designed uriedo-anilinophthalazine derivatives **7a-i** showed superior binding affinity than their anilinophthalazine parents in the VEGFR-2 kinase inhibition assay with  $IC_{50}$  ranged between 0.083 and 0.473  $\mu\text{M}$ . In particular, compounds **7g-i** showed  $IC_{50}$  values of 0.086, 0.083 and 0.086  $\mu\text{M}$ , respectively, which are better than that of the reference drug sorafenib ( $IC_{50} = 0.09 \mu\text{M}$ ). Our ultimate conclusion is that VEGFR-2 inhibitors with high binding affinity could be designed by extending the hydrophobic interaction between the inhibitor and the hydrophobic back pocket of the VEGFR-2 active site.

### 4. Experimental

#### 4.1. Chemistry

Melting points were measured with a Stuart melting point apparatus and were uncorrected. Infrared spectra were recorded as potassium bromide discs on Shimadzu FT-IR 8400S spectrophotometer and expressed in wave number ( $\text{cm}^{-1}$ ). The NMR spectra were recorded by Varian Gemini-300BB 300 MHz FT-NMR spectrometers (Varian Inc., Palo Alto, CA).  $^1\text{H}$  and  $^{13}\text{C}$  spectra were run at 300 and 75 MHz, respectively, in deuterated dimethylsulphoxide ( $\text{DMSO-}d_6$ ). Chemical shifts ( $\delta_{\text{H}}$ ) are reported relative to TMS as internal standard. All coupling constant ( $J$ ) values are given in hertz. Mass spectra were measured on a GCMS-QP1000 EX spectrometer at 70 e.V. Elemental analyses was carried out at the Regional Center for Mycology and Biotechnology, Al-Azhar University, Cairo, Egypt Analytical thin layer chromatography (TLC) on silica gel plates containing UV indicator was employed routinely to follow the course of reactions and to check the purity of products. All reagents and solvents were purified and dried by standard techniques.

##### 4.1.1. (Z)-3-(4-Methoxybenzylidene)isobenzofuran-1(3H)-one (**1**)

Compound **1** was prepared according to reported procedure [26] (m.p. 147-149 °C).

#### 4.1.2. 4-(4-Methoxybenzyl)phthalazin-1(2H)-one (**2**)

Compound **2** was prepared according to reported procedure [26] (m.p. 193-195 °C).

#### 4.1.3. 1-Chloro-4-(4-methoxybenzyl)phthalazine (**3**)

4-(4-Methoxybenzyl)phthalazin-1(2H)-one **2** (2.66 g, 0.01 mol) was added portion-wise to a cooled stirred mixture of phosphorus oxychloride (15 mL) and *N,N*-dimethylaniline (0.5 mL). After refluxing for 10 h, the reaction mixture was cooled then poured onto ice/water and alkalinized with 2 *N* NaOH. The aqueous solution was extracted three times with ethyl acetate. The combined organic extracts were dried over anhydrous Na<sub>2</sub>SO<sub>4</sub> then filtered, and the solvent was removed under reduced pressure. The obtained solid was crystallized from ethanol to give **3** (1.7 g, 60%) as beige solid; m.p. 187-189 °C; IR (KBr,  $\nu$  cm<sup>-1</sup>): <sup>1</sup>H NMR (DMSO-*d*<sub>6</sub>)  $\delta$  ppm: 3.68 (s, 3H, OCH<sub>3</sub>), 4.63 (s, 2H, CH<sub>2</sub>), 6.81 (d, 2H, H-3 and H-5 of 4-OCH<sub>3</sub>-C<sub>6</sub>H<sub>4</sub>, *J* = 8.7 Hz), 7.23 (d, 2H, H-2 and H-6 of 4-OCH<sub>3</sub>-C<sub>6</sub>H<sub>4</sub>, *J* = 9.0 Hz), 8.05 – 8.12 (m, 2H, H-6 and H-7 phthalazine), 8.25 – 8.29 (m, 1H, H-5 phthalazine), 8.34 – 8.37 (m, 1H, H-8 phthalazine).

#### 4.1.4. General procedure for preparation of target compounds (**4a-j**):

To a stirred solution of 1-chloro-4-(4-methoxybenzyl)phthalazine **3** (2.84 g, 0.01 mol) in refluxing acetone (15 mL), a solution of the appropriate aniline (0.012 mol) in acetone was added. The reaction mixture was heated under reflux for 3 h. The precipitate formed after cooling was collected by filtration and washed with water, dried then recrystallized from ethanol-dioxane mixture except **4j**, recrystallized from ethanol-DMF mixture.

##### 4.1.4.1. 4-(4-Methoxybenzyl)-*N*-phenylphthalazin-1-amine (**4a**):

Yellow crystals (yield 66%); m.p. 263-265 °C; IR (KBr,  $\nu$  cm<sup>-1</sup>): 3232 (NH), 2592 (CH aliphatic); <sup>1</sup>H NMR (DMSO-*d*<sub>6</sub>)  $\delta$  ppm: 3.68 (s, 3H, OCH<sub>3</sub>), 4.54 (s, 2H, CH<sub>2</sub>), 6.83 (d, 2H, H-3 and H-5 of 4-OCH<sub>3</sub>-C<sub>6</sub>H<sub>4</sub>, *J* = 8.7 Hz), 7.17 (t, 1H, H-4 of NH-C<sub>6</sub>H<sub>5</sub>, *J* = 7.8 Hz), 7.27 (d, 2H, H-2 and H-6 of 4-OCH<sub>3</sub>-C<sub>6</sub>H<sub>4</sub>, *J* = 8.1 Hz), 7.42 (t, 2H, H-3 and H-5 of NH-C<sub>6</sub>H<sub>5</sub>, *J* = 7.8 Hz), 7.81 (d, 2H, H-2 and H-6 of NH-C<sub>6</sub>H<sub>5</sub>, *J* = 7.2 Hz), 7.99 – 8.09 (m, 2H, H-6 and H-7 phthalazine), 8.25 (d, 1H, H-5 phthalazine, *J* = 7.8 Hz), 8.83 (d, 1H, H-8 phthalazine, *J* = 7.5 Hz), 10.17 (s, 1H, NH); <sup>13</sup>C NMR (DMSO-*d*<sub>6</sub>)  $\delta$  ppm: 36.19 (-CH<sub>2</sub>-), 55.01 (-OCH<sub>3</sub>), 114.00,

120.09, 122.31, 122.48, 123.99, 126.18, 126.43, 128.79, 129.62, 133.07, 133.33, 138.80, 152.23, 152.35, 157.93; Anal. Calcd. for C<sub>22</sub>H<sub>19</sub>N<sub>3</sub>O: C, 77.40; H, 5.61; N, 12.31; Found C, 77.61; H, 5.66; N, 12.53.

4.1.4.2. 4-(4-Methoxybenzyl)-N-(3-(trifluoromethyl)phenyl)phthalazin-1-amine (**4b**):

White crystals (yield 73%); m.p. 215-218 °C; IR (KBr,  $\nu$  cm<sup>-1</sup>): 3446 (NH), 2677 (CH aliphatic); <sup>1</sup>H NMR (DMSO-*d*<sub>6</sub>)  $\delta$  ppm: 3.67 (s, 3H, OCH<sub>3</sub>), 4.49 (s, 2H, CH<sub>2</sub>), 6.80 (d, 2H, H-3 and H-5 of 4-OCH<sub>3</sub>-C<sub>6</sub>H<sub>4</sub>, *J* = 8.1 Hz), 7.22 (d, 2H, H-2 and H-6 of 4-OCH<sub>3</sub>-C<sub>6</sub>H<sub>4</sub>, *J* = 8.7 Hz), 7.32 (d, 1H, H-4 of 3-CF<sub>3</sub>-C<sub>6</sub>H<sub>4</sub>, *J* = 7.8 Hz), 7.58 (t, 1H, H-5 of 3-CF<sub>3</sub>-C<sub>6</sub>H<sub>4</sub>, *J* = 7.8 Hz), 7.87 – 7.98 (m, 2H, H-6 and H-7 phthalazine), 8.12 (d, 1H, H-6 of 3-CF<sub>3</sub>-C<sub>6</sub>H<sub>4</sub>, *J* = 7.5 Hz), 8.25 (d, 1H, H-5 phthalazine, *J* = 8.4 Hz), 8.50 (s, 1H, H-2 of 3-CF<sub>3</sub>-C<sub>6</sub>H<sub>4</sub>), 8.58 (d, 1H, H-8 phthalazine, *J* = 7.8 Hz), 9.41 (s, 1H, NH); <sup>13</sup>C NMR (DMSO-*d*<sub>6</sub>)  $\delta$  ppm: 37.59 (-CH<sub>2</sub>-), 55.02 (-OCH<sub>3</sub>), 113.71, 113.99, 115.93, 117.80, 118.79, 122.58, 123.47, 125.25, 125.97, 126.91, 128.89, 129.32, 129.40, 129.48, 131.36, 131.96, 141.67, 151.74, 153.39, 157.70; Anal. Calcd. for C<sub>23</sub>H<sub>18</sub>F<sub>3</sub>N<sub>3</sub>O: C, 67.48; H, 4.43; N, 10.26; Found C, 67.59; H, 4.47; N, 10.52.

4.1.4.3. 4-((4-(4-Methoxybenzyl)phthalazin-1-yl)amino)benzonitrile (**4c**):

Yellow crystals (yield 68%); m.p. 247-249 °C; IR (KBr,  $\nu$  cm<sup>-1</sup>): 3244 (NH), 2630 (CH aliphatic), 2218 (C≡N); <sup>1</sup>H NMR (DMSO-*d*<sub>6</sub>)  $\delta$  ppm: 3.68 (s, 3H, OCH<sub>3</sub>), 4.64 (s, 2H, CH<sub>2</sub>), 6.83 (d, 2H, H-3 and H-5 of 4-OCH<sub>3</sub>-C<sub>6</sub>H<sub>4</sub>, *J* = 9.0 Hz), 7.30 (d, 2H, H-2 and H-6 of 4-OCH<sub>3</sub>-C<sub>6</sub>H<sub>4</sub>, *J* = 8.4 Hz), 7.83 (d, 2H, H-2 and H-6 of 4-CN-C<sub>6</sub>H<sub>4</sub>, *J* = 8.1 Hz), 8.03 – 8.16 (m, 4H, H-3, H-5 of 4-CN-C<sub>6</sub>H<sub>4</sub> and H-6, H-7 phthalazine), 8.34 (d, 1H, H-5 phthalazine, *J* = 8.1 Hz), 8.82 (d, 1H, H-8 phthalazine, *J* = 7.8 Hz), 10.27 (s, 1H, NH); <sup>13</sup>C NMR (DMSO-*d*<sub>6</sub>)  $\delta$  ppm: 35.73 (-CH<sub>2</sub>-), 54.85 (-OCH<sub>3</sub>), 104.34, 113.92, 114.20, 119.25, 120.51, 120.85, 121.12, 123.79, 124.00, 126.47, 129.21, 129.61, 129.72, 132.89, 133.06, 144.18, 152.42, 153.72, 158.04; MS *m/z* 366 [M<sup>+</sup>]; Anal. Calcd. for C<sub>23</sub>H<sub>18</sub>N<sub>4</sub>O: C, 75.39; H, 4.95; N, 15.29; Found C, 75.53; H, 5.01; N, 15.48.

4.1.4.4. N-(2-Chlorophenyl)-4-(4-methoxybenzyl)phthalazin-1-amine (**4d**):

Beige crystals (yield 59%); m.p. 155-157°C; IR (KBr,  $\nu$  cm<sup>-1</sup>): 3250 (NH), 2586 (CH aliphatic); <sup>1</sup>H NMR (DMSO-*d*<sub>6</sub>)  $\delta$  ppm: 3.67 (s, 3H, OCH<sub>3</sub>), 4.43 (s, 2H, CH<sub>2</sub>), 6.80 (d, 2H, H-3 and H-5 of 4-OCH<sub>3</sub>-C<sub>6</sub>H<sub>4</sub>, *J* = 8.7 Hz), 7.19 (d, 2H, H-2 and H-6 of 4-OCH<sub>3</sub>-C<sub>6</sub>H<sub>4</sub>, *J* = 8.7 Hz), 7.25 (d, 1H, H-3 of 2-Cl-C<sub>6</sub>H<sub>4</sub>, *J* = 7.8 Hz), 7.40 (t, 1H, H-4 of 2-Cl-C<sub>6</sub>H<sub>4</sub>, *J* = 8.4 Hz), 7.54 (d, 1H, H-6 of 2-Cl-C<sub>6</sub>H<sub>4</sub>, *J* = 7.8 Hz), 7.71 – 7.73 (m, 1H, H-5 of 2-Cl-C<sub>6</sub>H<sub>4</sub>), 7.88 – 7.96

(m, 2H, H-6 and H-7 phthalazine), 8.10 (d, 1H, H-5 phthalazine,  $J= 9.3$  Hz), 8.44 (d, 1H, H-8 phthalazine,  $J= 7.8$  Hz), 11.16 (s, 1H, NH, D<sub>2</sub>O exchangeable); Anal. Calcd. for C<sub>22</sub>H<sub>18</sub>ClN<sub>3</sub>O: C, 70.30; H, 4.83; N, 11.18; Found C, 70.54; H, 4.91; N, 11.36.

4.1.4.5. *N*-(3-Chlorophenyl)-4-(4-methoxybenzyl)phthalazin-1-amine (**4e**):

White crystals (yield 59%); m.p. 241-243 °C; IR (KBr,  $\nu$  cm<sup>-1</sup>): 3290 (NH), 2675 (CH aliphatic); <sup>1</sup>H NMR (DMSO-*d*<sub>6</sub>)  $\delta$  ppm: 3.68 (s, 3H, OCH<sub>3</sub>), 4.60 (s, 2H, CH<sub>2</sub>), 6.83 (d, 2H, H-3 and H-5 of 4-OCH<sub>3</sub>-C<sub>6</sub>H<sub>4</sub>,  $J= 8.1$  Hz), 7.20 (d, 1H, H-4 of 3-Cl-C<sub>6</sub>H<sub>4</sub>,  $J= 8.1$  Hz), 7.30 (d, 2H, H-2 and H-6 of 4-OCH<sub>3</sub>-C<sub>6</sub>H<sub>4</sub>,  $J= 8.7$  Hz), 7.44 (t, 1H, H-5 of 3-Cl-C<sub>6</sub>H<sub>4</sub>,  $J= 8.1$  Hz), 7.78 (d, 1H, H-6 of 3-Cl-C<sub>6</sub>H<sub>4</sub>,  $J= 8.1$  Hz), 8.04 – 8.15 (m, 3H, H-2 of 3-Cl-C<sub>6</sub>H<sub>4</sub> and H-6, H-7 phthalazine), 8.33 (d, 1H, H-5 phthalazine,  $J= 7.8$  Hz), 8.93 (d, 1H, H-8 phthalazine,  $J= 8.4$  Hz), 10.49 (s, 1H, NH); <sup>13</sup>C NMR (DMSO-*d*<sub>6</sub>)  $\delta$  ppm: 35.48 (-CH<sub>2</sub>-), 54.85 (-OCH<sub>3</sub>), 113.92, 114.19, 120.52, 121.71, 121.97, 123.83, 124.17, 124.36, 126.54, 129.02, 129.64, 129.75, 130.34, 133.02, 133.84, 140.29, 152.57, 152.82, 158.06; MS *m/z* 377 [(M+2)<sup>+</sup>], 375 [M<sup>+</sup>]; Anal. Calcd. for C<sub>22</sub>H<sub>18</sub>ClN<sub>3</sub>O: C, 70.30; H, 4.83; N, 11.18; Found C, 70.52; H, 4.90; N, 11.38.

4.1.4.6. *N*-(4-Chlorophenyl)-4-(4-methoxybenzyl)phthalazin-1-amine (**4f**):

Yellow crystals (yield 72%); m.p. 233-235°C; IR (KBr,  $\nu$  cm<sup>-1</sup>): 3334 (NH), 2594 (CH aliphatic); <sup>1</sup>H NMR (DMSO-*d*<sub>6</sub>)  $\delta$  ppm: 3.70 (s, 3H, OCH<sub>3</sub>), 4.61 (s, 2H, CH<sub>2</sub>), 6.85 (d, 2H, H-3 and H-5 of 4-OCH<sub>3</sub>-C<sub>6</sub>H<sub>4</sub>,  $J= 8.7$  Hz), 7.29 (d, 2H, H-2 and H-6 of 4-OCH<sub>3</sub>-C<sub>6</sub>H<sub>4</sub>,  $J= 8.7$  Hz), 7.52 (d, 2H, H-3 and H-5 of 4-Cl-C<sub>6</sub>H<sub>4</sub>,  $J= 8.7$  Hz), 7.78 (d, 2H, H-2 and H-6 of 4-Cl-C<sub>6</sub>H<sub>4</sub>,  $J= 8.7$  Hz), 8.10 – 8.21 (m, 2H, H-6 and H-7 phthalazine), 8.38 (d, 1H, H-5 phthalazine,  $J= 7.8$  Hz), 8.89 (d, 1H, H-8 phthalazine,  $J= 8.4$  Hz), 10.60 (s, 1H, NH, D<sub>2</sub>O exchangeable); Anal. Calcd. for C<sub>22</sub>H<sub>18</sub>ClN<sub>3</sub>O: C, 70.30; H, 4.83; N, 11.18; Found C, 70.51; H, 4.89; N, 11.34.

4.1.4.7. *N*-(4-Chloro-3-(trifluoromethyl)phenyl)-4-(4-methoxybenzyl)phthalazin-1-amine (**4g**):

White crystals (yield 67%); m.p. 240-242°C; IR (KBr,  $\nu$  cm<sup>-1</sup>): 3242 (NH), 2692 (CH aliphatic); <sup>1</sup>H NMR (DMSO-*d*<sub>6</sub>)  $\delta$  ppm: 3.69 (s, 3H, OCH<sub>3</sub>), 4.74 (s, 2H, CH<sub>2</sub>), 6.85 (d, 2H, H-3 and H-5 of 4-OCH<sub>3</sub>-C<sub>6</sub>H<sub>4</sub>,  $J= 8.7$  Hz), 7.35 (d, 2H, H-2 and H-6 of 4-OCH<sub>3</sub>-C<sub>6</sub>H<sub>4</sub>,  $J= 9.0$  Hz), 7.79 (d, 1H, H-5 of 4-Cl-3-CF<sub>3</sub>-C<sub>6</sub>H<sub>3</sub>,  $J= 8.7$  Hz), 8.15 – 8.28 (m, 3H, H-6 of 4-Cl-3-CF<sub>3</sub>-C<sub>6</sub>H<sub>3</sub> and H-6, H-7 phthalazine), 8.43 (s, 1H, H-2 of 4-Cl-3-CF<sub>3</sub>-C<sub>6</sub>H<sub>3</sub>), 8.48 (d, 1H, H-5 phthalazine,  $J= 8.4$  Hz), 9.14 (d, 1H, H-8 phthalazine,  $J= 8.4$  Hz), 11.15 (s, 1H, NH); <sup>13</sup>C NMR (DMSO-*d*<sub>6</sub>)  $\delta$  ppm: 34.13 (-CH<sub>2</sub>-), 54.97 (-OCH<sub>3</sub>), 114.14, 114.23, 120.89, 121.44,

122.11, 124.51, 125.03, 126.84, 127.73, 127.88, 129.89, 132.16, 134.63, 135.62, 137.54, 153.12, 153.31, 157.94, 158.29; Anal. Calcd. For  $C_{23}H_{17}ClF_3N_3O$ : C, 62.24; H, 3.86; N, 9.47; Found C, 62.39; H, 3.89; N, 9.63.

4.1.4.8. 4-(4-Methoxybenzyl)-N-(3-methoxyphenyl)phthalazin-1-amine (**4h**):

Yellow crystals (yield 60%); m.p. 157-159°C; IR (KBr,  $\nu$   $cm^{-1}$ ): 3419 (NH), 2927 (CH aliphatic);  $^1H$  NMR (DMSO- $d_6$ )  $\delta$  ppm: 3.69 (s, 3H, OCH<sub>3</sub>), 3.79 (s, 3H, OCH<sub>3</sub>), 4.62 (s, 2H, CH<sub>2</sub>), 6.85 – 6.88 (m, 3H, H-4 of 3-OCH<sub>3</sub>-C<sub>6</sub>H<sub>4</sub> and H-3 and H-5 of 4-OCH<sub>3</sub>-C<sub>6</sub>H<sub>4</sub>), 7.31 – 7.42 (m, 5H, H-2, H-5 and H-6 of 3-OCH<sub>3</sub>-C<sub>6</sub>H<sub>4</sub> and H-2 and H-6 of 4-OCH<sub>3</sub>-C<sub>6</sub>H<sub>4</sub>), 8.11 – 8.21 (m, 2H, H-6 and H-7 phthalazine), 8.38 (d, 1H, H-5 phthalazine,  $J$  = 8.1 Hz), 9.04 (d, 1H, H-8 phthalazine,  $J$  = 7.8 Hz), 10.89 (s, 1H, NH);  $^{13}C$  NMR (DMSO- $d_6$ )  $\delta$  ppm: 35.08 (-CH<sub>2</sub>-), 54.97 (-OCH<sub>3</sub>), 55.27 (-OCH<sub>3</sub>), 109.76, 111.42, 114.12, 116.01, 121.09, 124.96, 126.85, 127.15, 128.50, 129.80, 129.98, 134.59, 138.17, 152.27, 152.46, 158.15, 159.88; MS  $m/z$  371 [ $M^+$ ]; Anal. Calcd. for  $C_{23}H_{21}N_3O_2$ : C, 74.37; H, 5.70; N, 11.31; Found C, 74.55; H, 5.78; N, 11.53.

4.1.4.9. 4-(4-Methoxybenzyl)-N-(4-methoxyphenyl)phthalazin-1-amine (**4i**):

Yellow crystals (yield 64%); m.p. 243-245°C; IR (KBr,  $\nu$   $cm^{-1}$ ): 3273 (NH), 2619 (CH aliphatic);  $^1H$  NMR (DMSO- $d_6$ )  $\delta$  ppm: 3.69 (s, 3H, OCH<sub>3</sub>), 3.80 (s, 3H, OCH<sub>3</sub>), 4.51 (s, 2H, CH<sub>2</sub>), 6.83 (d, 2H, H-3 and H-5 of 4-OCH<sub>3</sub>-C<sub>6</sub>H<sub>4</sub>,  $J$  = 9.0 Hz), 7.02 (d, 2H, H-3 and H-5 of 4-OCH<sub>3</sub>-C<sub>6</sub>H<sub>4</sub>-NH,  $J$  = 9.3 Hz), 7.26 (d, 2H, H-2 and H-6 of 4-OCH<sub>3</sub>-C<sub>6</sub>H<sub>4</sub>,  $J$  = 8.4 Hz), 7.62 (d, 2H, H-2 and H-6 of 4-OCH<sub>3</sub>-C<sub>6</sub>H<sub>4</sub>-NH,  $J$  = 8.7 Hz), 8.01 – 8.10 (m, 2H, H-6 and H-7 phthalazine), 8.24 (d, 1H, H-5 phthalazine,  $J$  = 7.2 Hz), 8.87 (d, 1H, H-8 phthalazine,  $J$  = 7.5 Hz), 10.41 (s, 1H, NH);  $^{13}C$  NMR (DMSO- $d_6$ )  $\delta$  ppm: 36.18 (-CH<sub>2</sub>-), 54.94 (-OCH<sub>3</sub>), 55.27 (-OCH<sub>3</sub>), 113.96, 114.37, 120.26, 124.34, 125.39, 126.32, 126.58, 129.47, 129.64, 130.29, 133.17, 133.88, 151.86, 152.10, 156.96, 157.96; Anal. Calcd. for  $C_{23}H_{21}N_3O_2$ : C, 74.37; H, 5.70; N, 11.31; Found C, 74.53; H, 5.81; N, 11.52.

4.1.4.10. 4-((4-(4-Methoxybenzyl)phthalazin-1-yl)amino)benzenesulfonamide (**4j**):

White crystals (yield 70%); m.p. 251-253°C; IR (KBr,  $\nu$   $cm^{-1}$ ): 3406, 3325, 3259 (NH, NH<sub>2</sub>), 2644 (CH aliphatic), 1327, 1147 (SO<sub>2</sub>);  $^1H$  NMR (DMSO- $d_6$ )  $\delta$  ppm: 3.69 (s, 3H, OCH<sub>3</sub>), 4.64 (s, 2H, CH<sub>2</sub>), 6.85 (d, 2H, H-3 and H-5 of 4-OCH<sub>3</sub>-C<sub>6</sub>H<sub>4</sub>,  $J$  = 9.0 Hz), 7.30 (d, 2H, H-2 and H-6 of 4-OCH<sub>3</sub>-C<sub>6</sub>H<sub>4</sub>,  $J$  = 8.4 Hz), 7.86 (d, 2H, H-2 and H-6 of 4-SO<sub>2</sub>NH<sub>2</sub>-C<sub>6</sub>H<sub>4</sub>,  $J$  = 8.7 Hz), 7.99 (d, 2H, H-3 and H-5 of 4-SO<sub>2</sub>NH<sub>2</sub>-C<sub>6</sub>H<sub>4</sub>,  $J$  = 8.4 Hz), 8.08 – 8.21 (m, 2H, H-6 and H-7

phthalazine), 8.38 (d, 1H, H-5 phthalazine,  $J= 7.8$  Hz), 8.85 (d, 1H, H-8 phthalazine,  $J= 7.8$  Hz), 10.35 (s, 1H, NH, D<sub>2</sub>O exchangeable); Anal. Calcd. for C<sub>22</sub>H<sub>20</sub>N<sub>4</sub>O<sub>3</sub>S: C, 62.84; H, 4.79; N, 13.32; Found C, 62.97; H, 4.86; N, 13.47.

#### 4.1.5. substituted 1-(4-nitrophenyl)-3-phenylurea (**5a-i**)

Compounds **5a-i** were prepared according to reported procedures [35].

#### 4.1.6. substituted 1-(4-aminophenyl)-3-phenylurea (**6a-i**)

Compounds **6a-c, e, f, i** [35], **6g** [36] and **6h** [37] are previously reported.

##### 4.1.6.1. 1-(2-Chlorophenyl)-3-(4-aminophenyl)urea (**6d**):

White crystals (yield 69%); m.p. 209-211 °C; IR (KBr,  $\nu$  cm<sup>-1</sup>): 3489, 3394, 3305 (NH, NH<sub>2</sub>), 1631 (C=O); <sup>1</sup>H NMR (DMSO-*d*<sub>6</sub>)  $\delta$  ppm: 4.78 (s, 2H, NH<sub>2</sub>, D<sub>2</sub>O exchangeable), 6.53 (d, 2H, H-3 and H-5 of 4-NH<sub>2</sub>-C<sub>6</sub>H<sub>4</sub>-NH,  $J= 6.9$  Hz), 6.97 (t, 1H, H-4 of 2-Cl-C<sub>6</sub>H<sub>4</sub>,  $J= 7.5$  Hz), 7.07 (d, 2H, H-2 and H-6 of 4-NH<sub>2</sub>-C<sub>6</sub>H<sub>4</sub>-NH,  $J= 8.7$  Hz), 7.25 (t, 1H, H-5 of 2-Cl-C<sub>6</sub>H<sub>4</sub>,  $J= 7.8$  Hz), 7.39 (d, 1H, H-3 of 2-Cl-C<sub>6</sub>H<sub>4</sub>,  $J= 7.5$  Hz), 8.07 (s, 1H, NH<sub>urea</sub>, D<sub>2</sub>O exchangeable), 8.14 (d, 1H, H-6 of 2-Cl-C<sub>6</sub>H<sub>4</sub>,  $J= 8.4$  Hz), 8.90 (s, 1H, NH<sub>urea</sub>, D<sub>2</sub>O exchangeable).

#### 4.1.7. General procedure for preparation of target compounds (**7a-i**):

A solution of 1-chloro-4-(4-methoxybenzyl)phthalazine **3** (2.84 g, 0.01 mol) in acetone was added to a stirred solution of **6a-i** (0.01 mol) in refluxing acetone. The reaction mixture was refluxed for 2 h then left to cool. The precipitated solid was filtered, dried and recrystallized from dioxan to give **7a-i**.

##### 4.1.7.1. 1-(4-((4-(4-Methoxybenzyl)phthalazin-1-yl)amino)phenyl)-3-phenylurea (**7a**):

Yellow crystals (yield 65%); m.p. 250-253 °C; IR (KBr,  $\nu$  cm<sup>-1</sup>): 3253 (NH), 2922 (CH aliphatic), 1697 (C=O); <sup>1</sup>H NMR (DMSO-*d*<sub>6</sub>)  $\delta$  ppm: 3.70 (s, 3H, OCH<sub>3</sub>), 4.52 (s, 2H, CH<sub>2</sub>), 6.85 (d, 2H, H-3 and H-5 of 4-OCH<sub>3</sub>-C<sub>6</sub>H<sub>4</sub>,  $J= 8.7$  Hz), 6.97 (t, 1H, H-4 of NH-C<sub>6</sub>H<sub>5</sub>,  $J= 7.5$  Hz), 7.26 – 7.31 (m, 4H, H-3, H-5 of NH-C<sub>6</sub>H<sub>5</sub> and H-2, H-6 of 4-OCH<sub>3</sub>-C<sub>6</sub>H<sub>4</sub>), 7.46 – 7.53 (m, 4H, HN-C<sub>6</sub>H<sub>4</sub>-NH), 7.61 (d, 2H, H-2 and H-6 of NH-C<sub>6</sub>H<sub>5</sub>,  $J= 8.4$  Hz), 8.16 – 8.20 (m, 2H, H-6 and H-7 phthalazine), 8.36 (d, 1H, H-5 phthalazine,  $J= 9.0$  Hz), 8.85 (d, 1H, H-8 phthalazine,  $J= 9.3$  Hz), 9.12 (s, 1H, NH<sub>urea</sub>, D<sub>2</sub>O exchangeable), 9.30 (s, 1H, NH<sub>urea</sub>, D<sub>2</sub>O exchangeable), 10.88 (s, 1H, NH, D<sub>2</sub>O exchangeable); Anal. Calcd. for C<sub>29</sub>H<sub>25</sub>N<sub>5</sub>O<sub>2</sub>: C, 73.25; H, 5.30; N, 14.73; Found C, 73.41; H, 5.38 ; N, 14.91.

4.1.7.2. *1-(4-((4-(4-Methoxybenzyl)phthalazin-1-yl)amino)phenyl)-3-(3-(trifluoromethyl)phenyl)urea (7b)*:

Yellow crystals (yield 77%); m.p. 205-207 °C; IR (KBr,  $\nu$   $\text{cm}^{-1}$ ): 3282 (NH), 2933 (CH aliphatic), 1714 (C=O);  $^1\text{H}$  NMR (DMSO- $d_6$ )  $\delta$  ppm: 3.70 (s, 3H, OCH<sub>3</sub>), 4.54 (s, 2H, CH<sub>2</sub>), 6.85 (d, 2H, H-3 and H-5 of 4-OCH<sub>3</sub>-C<sub>6</sub>H<sub>4</sub>,  $J$ = 8.7 Hz), 7.28 (d, 2H, H-2 and H-6 of 4-OCH<sub>3</sub>-C<sub>6</sub>H<sub>4</sub>,  $J$ = 9.0 Hz), 7.49 – 7.65 (m, 7H, H-4, H-5 and H-6 of 3-CF<sub>3</sub>-C<sub>6</sub>H<sub>4</sub> and 4H of HN-C<sub>6</sub>H<sub>4</sub>-NH), 8.01 (s, 1H, H-2 of 3-CF<sub>3</sub>-C<sub>6</sub>H<sub>4</sub>), 8.12 – 8.20 (m, 2H, H-6 and H-7 phthalazine), 8.35 (d, 1H, H-5 phthalazine,  $J$ = 9.3 Hz), 8.92 (d, 1H, H-8 phthalazine,  $J$ = 9.0 Hz), 9.71 (s, 1H, NH<sub>urea</sub>), 9.91 (s, 1H, NH<sub>urea</sub>), 10.94 (s, 1H, NH);  $^{13}\text{C}$  NMR (DMSO- $d_6$ )  $\delta$  ppm: 35.60 (-CH<sub>2</sub>-), 54.88 (-OCH<sub>3</sub>), 113.94, 114.19, 117.85, 118.90, 121.03, 121.42, 122.37, 124.80, 124.96, 125.81, 126.95, 128.57, 129.30, 129.72, 129.84, 129.90, 134.05, 137.92, 138.56, 140.67, 152.00, 152.67, 158.13; MS  $m/z$  543 [ $\text{M}^+$ ]; Anal. Calcd. for C<sub>30</sub>H<sub>24</sub>F<sub>3</sub>N<sub>5</sub>O<sub>2</sub>: C, 66.29; H, 4.45; N, 12.88; Found C, 66.38; H, 4.49 ; N, 13.04.

4.1.7.3. *1-(4-Cyanophenyl)-3-(4-((4-(4-methoxybenzyl)phthalazin-1-yl)amino)phenyl)urea (7c)*:

Brown crystals (yield 65%); m.p. 241-243°C; IR (KBr,  $\nu$   $\text{cm}^{-1}$ ): 3251 (NH), 3034 (CH aliphatic), 2216 (C $\equiv$ N), 1716 (C=O);  $^1\text{H}$  NMR (DMSO- $d_6$ )  $\delta$  ppm: 3.70 (s, 3H, OCH<sub>3</sub>), 4.54 (s, 2H, CH<sub>2</sub>), 6.85 (d, 2H, H-3 and H-5 of 4-OCH<sub>3</sub>-C<sub>6</sub>H<sub>4</sub>,  $J$ = 9.0 Hz), 7.27 (d, 2H, H-2 and H-6 of 4-OCH<sub>3</sub>-C<sub>6</sub>H<sub>4</sub>,  $J$ = 8.1 Hz), 7.55 – 7.73 (m, 8H, 4H of 4-CN-C<sub>6</sub>H<sub>4</sub> and 4H of HN-C<sub>6</sub>H<sub>4</sub>-NH), 8.07 – 8.20 (m, 2H, H-6 and H-7 phthalazine), 8.35 (d, 1H, H-5 phthalazine,  $J$ = 7.2 Hz), 8.92 (d, 1H, H-8 phthalazine,  $J$ = 8.1 Hz), 9.79 (s, 1H, NH<sub>urea</sub>), 10.10 (s, 1H, NH<sub>urea</sub>), 10.97 (s, 1H, NH);  $^{13}\text{C}$  NMR (DMSO- $d_6$ )  $\delta$  ppm: 35.63 (-CH<sub>2</sub>-), 55.00 (-OCH<sub>3</sub>), 103.06, 114.07, 117.70, 118.99, 119.28, 121.01, 124.89, 125.82, 126.94, 127.04, 128.54, 129.79, 133.26, 134.22, 135.03, 138.29, 144.26, 152.02, 152.28, 158.13; MS  $m/z$  500 [ $\text{M}^+$ ]; Anal. Calcd. for C<sub>30</sub>H<sub>24</sub>N<sub>6</sub>O<sub>2</sub>: C, 71.99; H, 4.83; N, 16.79; Found C, 72.17; H, 4.89 ; N, 17.03.

4.1.7.4. *1-(2-Chlorophenyl)-3-(4-((4-(4-methoxybenzyl)phthalazin-1-yl)amino)phenyl)urea (7d)*:

Yellow crystals (yield 53%); m.p. 249-251 °C; IR (KBr,  $\nu$   $\text{cm}^{-1}$ ): 3255 (NH), 2945 (CH aliphatic), 1703 (C=O);  $^1\text{H}$  NMR (DMSO- $d_6$ )  $\delta$  ppm: 3.69 (s, 3H, OCH<sub>3</sub>), 4.53 (s, 2H, CH<sub>2</sub>), 6.84 (d, 2H, H-3 and H-5 of 4-OCH<sub>3</sub>-C<sub>6</sub>H<sub>4</sub>,  $J$ = 8.7 Hz), 7.03 (t, 1H, H-4 of 2-Cl-C<sub>6</sub>H<sub>4</sub>,  $J$ = 7.8 Hz), 7.27 – 7.32 (m, 3H, H-5 of 2-Cl-C<sub>6</sub>H<sub>4</sub> and H-2, H-6 of 4-OCH<sub>3</sub>-C<sub>6</sub>H<sub>4</sub>), 7.43 (d, 1H, H-3

of 2-Cl-C<sub>6</sub>H<sub>4</sub>,  $J= 8.4$  Hz), 7.58 – 7.65 (m, 4H, HN-C<sub>6</sub>H<sub>4</sub>-NH), 8.07 – 8.17 (m, 3H, H-6 of 2-Cl-C<sub>6</sub>H<sub>4</sub> and H-6, H-7 phthalazine), 8.31 (d, 1H, H-5 phthalazine,  $J= 8.1$  Hz), 8.60 (s, 1H, NH<sub>urea</sub>), 8.94 (d, 1H, H-8 phthalazine,  $J= 8.7$  Hz), 10.16 (s, 1H, NH<sub>urea</sub>), 10.89 (s, 1H, NH); <sup>13</sup>C NMR (DMSO-*d*<sub>6</sub>)  $\delta$  ppm: 35.80 (-CH<sub>2</sub>-), 55.00 (-OCH<sub>3</sub>), 114.04, 118.80, 120.76, 121.57, 122.28, 123.28, 124.75, 125.18, 126.76, 126.81, 127.41, 128.91, 129.17, 129.73, 130.42, 133.83, 134.56, 136.00, 138.01, 151.97, 152.05, 152.32, 158.07; MS  $m/z$  511 [(M+2)<sup>+</sup>] and 509 [M<sup>+</sup>]; Anal. Calcd. for C<sub>29</sub>H<sub>24</sub>ClN<sub>5</sub>O<sub>2</sub>: C, 68.30; H, 4.74; N, 13.73; Found C, 68.42; H, 4.78 ; N, 13.89.

**4.1.7.5. 1-(3-Chlorophenyl)-3-(4-((4-(4-methoxybenzyl)phthalazin-1-yl)amino)phenyl)urea (7e):**

Beige crystals (yield 59%); m.p. 225-227 °C; IR (KBr,  $\nu$  cm<sup>-1</sup>): 3261 (NH), 2956 (CH aliphatic), 1701 (C=O); <sup>1</sup>H NMR (DMSO-*d*<sub>6</sub>)  $\delta$  ppm: 3.68 (s, 3H, OCH<sub>3</sub>), 4.51 (s, 2H, CH<sub>2</sub>), 6.84 (d, 2H, H-3 and H-5 of 4-OCH<sub>3</sub>-C<sub>6</sub>H<sub>4</sub>,  $J= 8.7$  Hz), 6.98 – 7.03 (m, 1H, H-4 of 3-Cl-C<sub>6</sub>H<sub>4</sub>), 7.26 – 7.31 (m, 4H, H-5, H-6 of 3-Cl-C<sub>6</sub>H<sub>4</sub> and H-2, H-6 of 4-OCH<sub>3</sub>-C<sub>6</sub>H<sub>4</sub>), 7.56 – 7.62 (m, 4H, HN-C<sub>6</sub>H<sub>4</sub>-NH), 7.72 (s, 1H, H-2 of 3-Cl-C<sub>6</sub>H<sub>4</sub>), 8.06 – 8.14 (m, 2H, H-6 and H-7 phthalazine), 8.29 (d, 1H, H-5 phthalazine,  $J= 6.9$  Hz), 8.83 (d, 1H, H-8 phthalazine,  $J= 6.9$  Hz), 9.53 (s, 1H, NH<sub>urea</sub>), 9.63 (s, 1H, NH<sub>urea</sub>), 10.61 (s, 1H, NH); <sup>13</sup>C NMR (DMSO-*d*<sub>6</sub>)  $\delta$  ppm: 36.06 (-CH<sub>2</sub>-), 54.99 (-OCH<sub>3</sub>), 114.02, 116.30, 117.22, 118.80, 120.59, 121.23, 124.45, 125.01, 126.62, 126.75, 129.07, 129.70, 130.33, 130.58, 133.16, 133.61, 134.40, 137.76, 141.39, 152.00, 152.54, 158.05; Anal. Calcd. for C<sub>29</sub>H<sub>24</sub>ClN<sub>5</sub>O<sub>2</sub>: C, 68.30; H, 4.74; N, 13.73; Found C, 68.47; H, 4.76 ; N, 13.86.

**4.1.7.6. 1-(4-Chlorophenyl)-3-(4-((4-(4-methoxybenzyl)phthalazin-1-yl)amino)phenyl)urea (7f):**

Beige crystals (yield 68%); m.p. 223-225 °C; IR (KBr,  $\nu$  cm<sup>-1</sup>): 3244 (NH), 2819 (CH aliphatic), 1674 (C=O); <sup>1</sup>H NMR (DMSO-*d*<sub>6</sub>)  $\delta$  ppm: 3.68 (s, 3H, OCH<sub>3</sub>), 4.51 (s, 2H, CH<sub>2</sub>), 6.83 (d, 2H, H-3 and H-5 of 4-OCH<sub>3</sub>-C<sub>6</sub>H<sub>4</sub>,  $J= 8.7$  Hz), 7.26 – 7.33 (m, 4H, H-2, H-6 of 4-OCH<sub>3</sub>-C<sub>6</sub>H<sub>4</sub> and H-3, H-5 of 4-Cl-C<sub>6</sub>H<sub>4</sub>), 7.48 – 7.62 (m, 6H, H-2, H-6 of 4-Cl-C<sub>6</sub>H<sub>4</sub> and 4H of HN-C<sub>6</sub>H<sub>4</sub>-NH), 8.07 – 8.15 (m, 2H, H-6 and H-7 phthalazine), 8.30 (d, 1H, H-5 phthalazine,  $J= 6.9$  Hz), 8.89 (d, 1H, H-8 phthalazine,  $J= 6.9$  Hz), 9.64 (s, 1H, NH<sub>urea</sub>), 9.66 (s, 1H, NH<sub>urea</sub>), 10.85 (s, 1H, NH); <sup>13</sup>C NMR (DMSO-*d*<sub>6</sub>)  $\delta$  ppm: 35.85 (-CH<sub>2</sub>-), 55.00 (-OCH<sub>3</sub>), 114.04, 118.71, 119.35, 120.78, 124.71, 125.12, 125.39, 126.79, 126.84, 128.56,

128.82, 129.75, 129.92, 133.86, 134.69, 138.33, 138.84, 151.97, 152.61, 158.08; Anal. Calcd. for C<sub>29</sub>H<sub>24</sub>ClN<sub>5</sub>O<sub>2</sub>: C, 68.30; H, 4.74; N, 13.73; Found C, 68.44; H, 4.76 ; N, 13.85.

**4.1.7.7. 1-(4-Chloro-3-(trifluoromethyl)phenyl)-3-(4-((4-(4-methoxybenzyl)phthalazin-1-yl)amino)phenyl)urea (7g):**

Orange crystals (yield 66%); m.p. 268-270 °C; IR (KBr,  $\nu$  cm<sup>-1</sup>): 3340 (NH), 2833 (CH aliphatic), 1714 (C=O); <sup>1</sup>H NMR (DMSO-*d*<sub>6</sub>)  $\delta$  ppm: 3.70 (s, 3H, OCH<sub>3</sub>), 4.52 (s, 2H, CH<sub>2</sub>), 6.85 (d, 2H, H-3 and H-5 of 4-OCH<sub>3</sub>-C<sub>6</sub>H<sub>4</sub>, *J* = 8.7 Hz), 7.26 (d, 2H, H-2 and H-6 of 4-OCH<sub>3</sub>-C<sub>6</sub>H<sub>4</sub>, *J* = 8.4 Hz), 7.53 – 7.68 (m, 6H, H-5, H-6 of 4-Cl-3-CF<sub>3</sub>-C<sub>6</sub>H<sub>3</sub> and 4H of HN-C<sub>6</sub>H<sub>4</sub>-NH), 8.08 – 8.17 (m, 3H, H-2 of 4-Cl-3-CF<sub>3</sub>-C<sub>6</sub>H<sub>3</sub> and H-6, H-7 phthalazine), 8.32 (d, 1H, H-5 phthalazine, *J* = 6.6 Hz), 8.83 (d, 1H, H-8 phthalazine, *J* = 6.6 Hz), 9.50 (s, 1H, NH<sub>urea</sub>), 9.84 (s, 1H, NH<sub>urea</sub>), 10.67 (s, 1H, NH); <sup>13</sup>C NMR (DMSO-*d*<sub>6</sub>)  $\delta$  ppm: 36.11 (-CH<sub>2</sub>-), 54.99 (-OCH<sub>3</sub>), 114.02, 116.41, 119.04, 120.52, 120.98, 122.10, 122.70, 124.32, 124.60, 124.84, 126.58, 126.72, 129.15, 129.69, 132.00, 133.56, 134.32, 137.32, 139.45, 152.06, 152.53, 158.04; Anal. Calcd. for C<sub>30</sub>H<sub>23</sub>ClF<sub>3</sub>N<sub>5</sub>O<sub>2</sub>: C, 62.34; H, 4.01; N, 12.12; Found C, 62.48; H, 4.07 ; N, 12.31.

**4.1.7.8. 1-(4-((4-(4-Methoxybenzyl)phthalazin-1-yl)amino)phenyl)-3-(3-methoxyphenyl)urea (7h):**

Beige crystals (yield 70%); m.p. 220-222 °C; IR (KBr,  $\nu$  cm<sup>-1</sup>): 3261 (NH), 2831 (CH aliphatic), 1683 (C=O); <sup>1</sup>H NMR (DMSO-*d*<sub>6</sub>)  $\delta$  ppm: 3.67 (s, 3H, OCH<sub>3</sub>), 3.74 (s, 3H, OCH<sub>3</sub>), 4.45 (s, 2H, CH<sub>2</sub>), 6.53 (d, 1H, H-4 of 3-OCH<sub>3</sub>-C<sub>6</sub>H<sub>4</sub>, *J* = 7.8 Hz), 6.80 (d, 2H, H-3 and H-5 of 4-OCH<sub>3</sub>-C<sub>6</sub>H<sub>4</sub>, *J* = 9.0 Hz), 6.92 (d, 1H, H-6 of 3-OCH<sub>3</sub>-C<sub>6</sub>H<sub>4</sub>, *J* = 7.2 Hz), 7.14 – 7.24 (m, 4H, H-2, H-5 of 3-OCH<sub>3</sub>-C<sub>6</sub>H<sub>4</sub> and H-2, H-6 of 4-OCH<sub>3</sub>-C<sub>6</sub>H<sub>4</sub>), 7.42 (d, 2H, HN-C<sub>6</sub>H<sub>4</sub>-NH, *J* = 8.7 Hz), 7.81 (d, 2H, HN-C<sub>6</sub>H<sub>4</sub>-NH, *J* = 8.7 Hz), 7.86 – 7.94 (m, 2H, H-6 and H-7 phthalazine), 8.07 (d, 1H, H-5 phthalazine, *J* = 6.3 Hz), 8.54 – 8.57 (m, 2H, H-8 phthalazine and NH<sub>urea</sub>), 8.63 (s, 1H, NH<sub>urea</sub>, D<sub>2</sub>O exchangeable), 9.02 (s, 1H, NH, D<sub>2</sub>O exchangeable); Anal. Calcd. for C<sub>30</sub>H<sub>27</sub>N<sub>5</sub>O<sub>3</sub>: C, 71.27; H, 5.38; N, 13.85; Found C, 71.52; H, 5.42; N, 14.02.

**4.1.7.9. 1-(4-((4-(4-Methoxybenzyl)phthalazin-1-yl)amino)phenyl)-3-(4-methoxyphenyl)urea (7i):**

Yellow crystals (yield 69%); m.p. 215-217 °C; IR (KBr,  $\nu$  cm<sup>-1</sup>): 3259 (NH), (CH aliphatic), 1666 (C=O); <sup>1</sup>H NMR (DMSO-*d*<sub>6</sub>)  $\delta$  ppm: 3.69 (s, 3H, 4-OCH<sub>3</sub>), 3.71 (s, 3H, 4-OCH<sub>3</sub>), 4.52 (s, 2H, CH<sub>2</sub>), 6.84 (d, 4H, H-3, H-5 of 4-OCH<sub>3</sub>-C<sub>6</sub>H<sub>4</sub>-CH<sub>2</sub> and H-3, H-5 of 4-OCH<sub>3</sub>-C<sub>6</sub>H<sub>4</sub>-NH

$J = 8.4$  Hz), 7.27 (d, 2H, H-2 and H-6 of 4-OCH<sub>3</sub>-C<sub>6</sub>H<sub>4</sub>,  $J = 8.1$  Hz), 7.37 (d, 2H, H-2 and H-6 of 4-OCH<sub>3</sub>-C<sub>6</sub>H<sub>4</sub>-NH,  $J = 8.7$  Hz), 7.52 – 7.61 (m, 4H, HN-C<sub>6</sub>H<sub>4</sub>-NH), 8.09 – 8.17 (m, 2H, H-6 and H-7 phthalazine), 8.31 (d, 1H, H-5 phthalazine,  $J = 8.4$  Hz), 8.91 (d, 1H, H-8 phthalazine,  $J = 6.9$  Hz), 9.16 (s, 1H, NH<sub>urea</sub>), 9.47 (s, 1H, NH<sub>urea</sub>), 10.94 (s, 1H, NH); <sup>13</sup>C NMR (DMSO-*d*<sub>6</sub>)  $\delta$  ppm: 35.82 (-CH<sub>2</sub>-), 55.00 (-OCH<sub>3</sub>), 55.14 (-OCH<sub>3</sub>), 113.97, 114.05, 118.55, 119.66, 120.87, 124.81, 125.55, 126.88, 128.77, 129.29, 129.76, 132.87, 133.94, 134.83, 138.97, 151.94, 152.88, 154.35, 158.10; Anal. Calcd. for C<sub>30</sub>H<sub>27</sub>N<sub>5</sub>O<sub>3</sub>: C, 71.27; H, 5.38; N, 13.85; Found C, 71.51; H, 5.44; N, 13.97.

#### 4.2. Measurement of inhibitory activity against VEGFR-2

The kinase activity of VEGFR-2 was carried out in the National Research Centre, Giza, Egypt and measured by use of an anti-phosphotyrosine antibody with the Alpha Screen system (PerkinElmer, USA) according to manufacturer's instructions. Enzyme reactions were performed in 50 mM Tris-HCl pH 7.5, 5 mM MnCl<sub>2</sub>, 5 mM MgCl<sub>2</sub>, 0.01% Tween-20 and 2 mM DTT, containing 10  $\mu$ M ATP, 0.1  $\mu$ g/mL biotinylated poly-GluTyr (4:1) and 0.1 nM of VEGFR-2 (Millipore, UK). Prior to catalytic initiation with ATP, the tested compounds at final concentrations ranging from 0-100  $\mu$ g/mL and enzyme were incubated for 5 min at room temperature. The reactions were quenched by the addition of 25  $\mu$ L of 100 mM EDTA, 10  $\mu$ g/mL Alpha Screen streptavidine donor beads and 10  $\mu$ g/mL acceptor beads in 62.5 mM HEPES pH 7.4, 250 mM NaCl, and 0.1% BSA. Plate was incubated in the dark overnight and then read by ELISA Reader (PerkinElmer, USA). Wells containing the substrate and the enzyme without compounds were used as reaction control. Wells containing biotinylated poly-GluTyr (4:1) and enzyme without ATP were used as basal control. Percent inhibition was calculated by the comparison of compounds treated to control incubations. The concentration of the test compound causing 50% inhibition (IC<sub>50</sub>) was calculated from the concentration-inhibition response curve (triplicate determinations) and the data were compared with Sorafenib as standard VEGFR-2 inhibitor.

#### 4.3. Molecular Docking study

All the molecular modeling studies were carried out using Molecular Operating Environment (MOE, 10.2008) software. All minimizations were performed with MOE until an RMSD gradient of 0.05 kcal·mol<sup>-1</sup>Å<sup>-1</sup> with MMFF94x force field and the partial charges were automatically calculated. The X-ray crystallographic structure of VEGFR-2 co-

crystallized with sorafenib as inhibitor (PDB ID: 4ASD) [38] was downloaded from the protein data bank [39]. The receptor was prepared for docking study using *Protonate 3D* protocol in MOE with default options followed by water molecules removal. The co-crystallized ligand was used to define the active site for docking. Triangle Matcher placement method and London dG scoring function were used for docking. Docking setup was first validated by re-docking of the co-crystallized ligand (Sorafenib) in the vicinity of the active site of the receptor with energy score (S) = -15.19 kcal/mol and RMSD of 0.470Å. The validated setup was then used in predicting the ligands receptor interactions at the active site for the synthesized and designed compounds.

#### 4.4. *In vitro* cytotoxic activity

The cytotoxicity assays were performed at National Cancer Institute (NCI), Bethesda, USA (against 60 cell lines). The human tumor cell lines of the cancer screening panel were grown in RPMI 1640 medium containing 5% fetal bovine serum and 2 mM L-glutamine. For a typical screening experiment, cells were inoculated into 96 well microtiter plates in 100  $\mu$ l at plating densities ranging from 5000 to 40,000 cells/well depending on the doubling time of individual cell lines. After cell inoculation, the microtiter plates were incubated at 37 °C, 5% CO<sub>2</sub>, 95% air and 100% relative humidity for 24 h prior to addition of experimental drugs. After 24 h, two plates of each cell line were fixed *in situ* with trichloroacetic acid (TCA), to represent a measurement of the cell population for each cell line at the time of drug addition ( $T_0$ ). Experimental drugs were solubilized in dimethyl sulfoxide at 400-fold the desired final maximum test concentration and stored frozen prior to use. At the time of drug addition, an aliquot of frozen concentrate was thawed and diluted to twice the desired final maximum test concentration with complete medium containing 50  $\mu$ g/ml gentamicin. Aliquot of 100  $\mu$ l of the drug dilution was added to the appropriate microtiter wells already containing 100  $\mu$ l of medium, resulting in the required final drug concentration (10  $\mu$ M). Triplicate wells were prepared for each individual dose. Following drug addition, the plates were incubated for an additional 48 h at 37 °C, 5% CO<sub>2</sub>, 95% air, and 100% relative humidity. For adherent cells, the assay was terminated by the addition of cold TCA. Cells were fixed *in situ* by the gentle addition of 50  $\mu$ l of cold 50% (w/v) TCA (final concentration, 10% TCA) and incubated for 60 min at 4 °C. The supernatant was discarded, and the plates were washed five times with tap water and air dried. Sulforhodamine B (SRB) solution (100  $\mu$ l) at 0.4% (w/v) in 1% acetic acid was added to each well, and plates were incubated for 10 min at room temperature. After

staining, unbound dye was removed by washing five times with 1% acetic acid and the plates were air dried. Bound stain was subsequently solubilized with 10 mM trizma base, and the absorbance was read on an automated plate reader at a wavelength of 515 nm. For suspension cells, the methodology was the same except that the assay was terminated by fixing settled cells at the bottom of the wells by gently adding 50  $\mu$ l of 80% TCA (final concentration, 16% TCA). Using the seven absorbance measurements [time zero ( $T_z$ ), control growth ( $C$ ), and test growth in the presence of drug ( $T_i$ )], the percentage growth was calculated at the drug concentration level. Percentage growth inhibition was calculated as:

$$[(T_i - T_z) / (C - T_z)] \times 100 \text{ for concentrations for which } T_i \geq T_z$$

$$[(T_i - T_z) / T_z] \times 100 \text{ for concentrations for which } T_i < T_z$$

### Acknowledgment

The authors would like to extend their sincere appreciation to the Deanship of Scientific Research at King Saud University for its funding of this research through the Research Group Project no. RGP-1436-038. Department of Pharmaceutical Chemistry, Faculty of Pharmacy, Cairo University, Cairo, Egypt, is highly appreciated for supporting this research. The authors are grateful to National Cancer Institute (NCI) Developmental Therapeutic Program ([www.dtp.nci.nih.gov](http://www.dtp.nci.nih.gov)) for screening the anticancer activity of the newly synthesized compounds in vitro.

3D Molecular graphics in the discussion and results section were generated using the UCSF Chimera package [40]. Chimera is developed by the Resource for Biocomputing, Visualization, and Informatics at the University of California, San Francisco, supported by grants from the National Institutes of Health National Center for Research Resources (2P41RR001081) and National Institute of General Medical Sciences (9P41GM103311).

### References

- [1] M. W. Dewhirst, Y. Cao and G. Vlahovic, In *Cancer Drug Discovery and Development: Antiangiogenic agents in cancer therapy*; B. A. Teicher, L. M. Ellis, Ed., Humana Press: Totowa, NJ, USA, Second edition 2007, Chapter 2, pp 27–47.
- [2] P. Carmeliet and R. K. Jain, *Nature* 2000, **407**, 249–257.
- [3] J. Folkman, *N. Engl. J. Med.* 1971, **285**, 1182–1186.
- [4] P. Carmeliet, *Nat. Med.* 2000, **6**, 389–395.

- [5] R. R. Jr., *Crit. Rev. Oncol. Hematol.* 2007, **62**, 179–213.
- [6] A.-K. Olsson, A. Dimberg, J. Kreuger and L. Claesson-Welsh, *Nat. Rev. Mol. Cell Biol.* 2006, **7**, 359–371.
- [7] N. Ferrara, H. P. Gerber and J. LeCouter, *Nat. Med.* 2003, **9**, 669–676.
- [8] P. Wu, T. E. Nielsen and M. H. Clausen, *Trends Pharmacol. Sci.* 2015, **36**, 422–439.
- [9] K. Miller-Moslin, S. Peukert, R. K. Jain, M. A. McEwan, R. Karki, L. Llamas, N. Yusuff, F. He, Y. Li, Y. Sun, M. Dai, L. Perez, W. Michael, T. Sheng, H. Lei, R. Zhang, J. Williams, A. Bourret, A. Ramamurthy, J. Yuan, R. Guo, M. Matsumoto, A. Vattay, W. Maniara, A. Amaral, M. Dorsch and J. F. Kelleher, *J. Med. Chem.* 2009, **52**, 3954–3968.
- [10] S. Zhang, Y. Zhao, Y. Liu, D. Chen, W. Q. Zhao, C. Dong, L. Xia and P. Gong, *Eur. J. Med. Chem.* 2010, **45**, 3504–3510.
- [11] M. Payton, T. L. Bush and G. Chung, *Cancer Res.* 2010, **70**, 9846–9854.
- [12] B. S. Lucas, W. Aaron, S. An, R. J. Austin, M. Brown, H. Chan, A. Chong, R. Hungate, T. Huang, B. Jiang, M. G. Johnson, J. A. Kaizerman, G. Lee, D. L. McMinn, J. Orf, J. P. Powers, M. Rong, M. M. Toteva, C. Uyeda, D. Wickramasinghe, G. Xu, Q. Ye and W. Zhong, *Bioorg. Med. Chem. Lett.* 2010, **20**, 3618–3622.
- [13] V. J. Cee, L. B. Schenkel, B. L. Hodous, H. L. Deak, H. N. Nguyen, P.R. Olivieri, K. Romero, A. Bak, X. Be, S. Bellon, T. L. Bush, A. C. Cheng, G. Chung, S. Coats, P. M. Eden, K. Hanestad, P. L. Gallant, Y. Gu, X. Huang, R. L. Kendall, M. J. Lin, M. J. Morrison, V. F. Patel, R. Radinsky, P. E. Rose, S. Ross, J. Sun, J. Tang, H. Zhao, M. Payton and S. D. Geuns-Meyer, *J. Med. Chem.* 2010, **53**, 6368–6377.
- [14] W. M. Eldehna, H. S. Ibrahim, H. A. Abdel-Aziz, N. N. Farrag and M. M. Youssef, *Eur. J. Med. Chem.* 2015, **89**, 549–560.
- [15] G. Bold, J. Frei, P. Traxler, K.-H. Altmann, H. Mett, D. R. Stover and J. M. Wood, EP Patent, 1998, 98/00764.
- [16] G. Bold, K.-H. Altmann, J. Frei, M. Lang, P. W. Manley, P. Traxler, B. Wietfeld, J. Brüggén, E. Buchdunger, R. Cozens, S. Ferrari, P. Furet, F. Hofmann, G. Martiny-Baron, J. Mestan, J. Rösel, M. Sills, D. Stover, F. Acemoglu, E. Boss, R. Emmenegger, L. Lässer, E. Masso, R. Roth, C. Schlachter, W. Vetterli, D. Wyss and J. M. Wood, *J. Med. Chem.* 2000, **43**, 2310–2323.
- [17] H. Joensuu, F. D. Braud, G. Grignagni, T. D. Pas, G. Spitalieri, P. Coco, C. Spreafico, S. Boselli, F. Toffalorio, P. Bono, T. Jalava, C. Kappeler, M. Aglietta, D. Laurent and P. G. Casali, *Br. J. Cancer* 2011, **104**, 1686–1690.

- [18] T. C. Gauler, B. Besse, A. Mauguen, J. B. Meric, V. Gounant, B. Fischer, T. R. Overbeck, H. Krissel, D. Laurent, M. Tiainen, F. Commo, J. C. Soria and W. E. E. Eberhardt, *Ann. Oncol.* 2012, **23**, 678–687.
- [19] T. Dragovich, D. Laheru, F. Dayyani, V. Bolejack, L. Smith, J. Seng, H. Burris, P. Rosen, M. Hidalgo, P. Ritch, A. F. Baker, N. Raghunand, J. Crowley and D. D. Von Hoff, *Cancer Chemother. Pharmacol.* 2014, **74**, 379–387.
- [20] J. Dumas and J. A. Dixon, *Expert Opin. Ther. Patents* 2005, **15**, 647–658.
- [21] E. L. Piatnitski, M. A. J. Duncton, A. S. Kiselyov, R. Katoch-Rouse, D. Sherman, D. L. Milligan, C. Balagtas, W. C. Wong, J. Kawakamia and J. F. Doody, *Bioorg. Med. Chem. Lett.* 2005, **15**, 4696–4698.
- [22] M. A. J. Duncton, E. L. Piatnitski, R. Katoch-Rouse, L. M. Smith, A. S. Kiselyov, D. L. Milligan, C. Balagtas, W. C. Wong, J. Kawakamia and J. F. Doody, *Bioorg. Med. Chem. Lett.* 2006, **16**, 1579–1581.
- [23] A. S. Kiselyov, V. V. Semenov and D. Milligan, *Chem. Biol. Drug Des.* 2006, **68**, 308–313.
- [24] M. A. J. Duncton, E. L. P. Chekler, R. Katoch-Rouse, D. Sherman, W. C. Wong, L. M. Smith, J. K. Kawakami, A. S. Kiselyov, D. L. Milligan, C. Balagtas, Y. R.; Hadari, Y. Wang, S. N. Patel, R. L. Rolster, J. R. Tonra, D. Surguladze, S. Mitelman, P. Kussie, P. Bohlen and J. F. Doody, *Bioorg. Med. Chem.* 2009, **17**, 731–740.
- [25] A. Papakyriakou, M. E. Katsarou, M. Belimezi, M. Karpusas and D. Vourloumis, *ChemMedChem.* 2010, **5**, 118–129.
- [26] H. S. Ibrahim, W. M. Eldehna, H. A. Abdel-Aziz, M. M. Elaasser and M. M. Abdel-Aziz, *Eur. J. Med. Chem.* 2014, **85**, 480–486.
- [27] Y. Oguro, N. Miyamoto, K. Okada, T. Takagi, H. Iwata, Y. Awazu, H. Miki, A. Hori, K. Kamiyama and S. Imamura, *Bioorg. Med. Chem.* 2010, **18**, 7260–7273.
- [28] L. Lintnerová, M. García-Caballero, F. Gregáň, M. Melicherčík, A. R. Quesada, J. Dobiaš, J. Lác, M. Sališová and A. A. Boháč, *Eur. J. Med. Chem.* 2014, **72**, 146–159.
- [29] M. McTigue, B. W. Murray, J. H. Chen, Y. L. Deng, J. Solowiej and R. S. Kania, *Proc. Natl. Acad. Sci. U S A.* 2012, **109**, 18281–18289.
- [30] H. Q. Li, P. C. Lv, T. Yan and H. L. Zhu, *Anticancer Agents Med. Chem.* 2009, **9**, 471–480.
- [31] A. Monks, D. Scudiero, P. Skehan, R. Shoemaker, K. Paull, D. Vistica, C. Hose, J. Langley, P. Cronise, A. Vaigro-Wolfe, M. Gray-Goodrich, H. Campbell and M. R. Boyd, *J. Natl. Cancer Inst.* 1991, **83**, 757–766.

- [32] M. R. Boyd and K. D. Paull, *Drug Develop. Res.* 1995, **34**, 91–109.
- [33] M. R. Boyd, In *Cancer Drug Discovery and Development: Anticancer Drug Development Guide: Preclinical Screening, Clinical Trials and Approval*; B. A., Teicher, Ed. Humana Press: Totowa, NJ, USA, Second edition 2014, Chapter 1, pp 41–62.
- [34] P. Skehan, R. Storeng, D. Scudiero, A. Monks, J. McMahon, D. Vistica, J. Warren, H. Bokesch, S. Kenney and M. Boyd, *J. Natl. Cancer Inst.* 1990, **82**, 1107–1112.
- [35] W. M. Eldehna, M. Fares, H. S. Ibrahim, M. H. Aly, S. Zada, M. M. Ali, S. M. Abou-Seri, H. A. Abdel-Aziz and D. A. A. El Ella, *Eur. J. Med. Chem.* 2015, **100**, 89–97.
- [36] Q. Zhang, Y. Diao, F. Wang, Y. Fu, F. Tang, Q. You and H. Zhou, *MedChemComm.* 2013, **4**, 979–986.
- [37] L. L. Yang, G. B. Li, S. Ma, C. Zou, S. Zhou, Q. Z. Sun, C. Cheng, X. Chen, L. J. Wang, S. Feng, L. L. Li and S. Y. Yang, *J. Med. Chem.* 2013, **56**, 1641–1655.
- [38] M. McTigue, B. W. Murray, J. H. Chen, Y. L. Deng, J. Solowiej and R. S. Kania, *Proc. Natl. Acad. Sci. U S A.* 2012, **109**, 18281–18289.
- [39] <http://www.rcsb.org/>
- [40] E. F. Pettersen, T. D. Goddard, C. C. Huang, G. S. Couch, D. M. Greenblatt, E. C. Meng and T. E. Ferrin, *J. Comput. Chem.* 2004, **25**, 1605–1612.

**FIGURE CAPTIONS**

**Figure 1.** Structures of VEGFR-2 inhibitors (**I-III**) and the target phthalazines **4a-j** and **7a-i**.

**Figure 2.** 2D schematic diagram representing vatalanib plausible binding mode in the VEGFR-2 active site.

**Figure 3.** (A) Superimposition of the co-crystallized (blue) and the docking pose (red) of sorafenib in the VEGFR-2 active site with RMSD of 0.470Å. (B) 2D interaction diagram showing sorafenib docking pose interactions with the key amino acids in the VEGFR-2 active site. (Distances in Å)

**Figure 4.** 2D diagram (A) and 3D representation (B) of compound **4g** showing its interaction with the VEGFR-2 receptor active site.

**Figure 5.** 2D diagram (A) and 3D representation (B) for compound **4j** showing its interaction with the VEGFR-2 receptor active site.

**Figure 6.** 2D diagram (A) and 3D representation (B) for compound **7h** showing its interaction with the VEGFR-2 receptor active site.

**Figure 7.** The most sensitive cell lines towards the target compounds **4a-j** and **7a-i** according to the GI %.

**TABLE CAPTIONS**

**Table 1.** VEGFR-2 kinase inhibitory activity of the synthesized compounds.

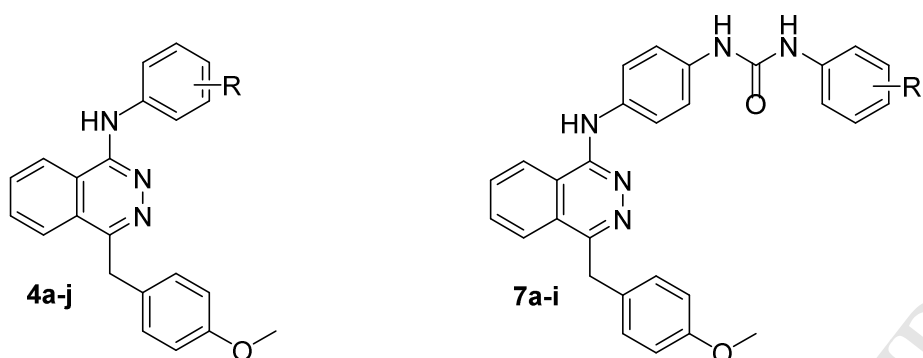
**Table 2.** Docking energy scores (S) in kcal/mol for compounds **4** and **7**.

**Table 3.** Percentage growth inhibition (GI %) of *in-vitro* subpanel tumor cell lines at 10 µM concentration for seventeen compounds.

**SCHEME CAPTIONS**

**Scheme 1.** Reagents and conditions: (i) CH<sub>3</sub>COONa / heating 200 °C 5 h; (ii) NH<sub>2</sub>NH<sub>2</sub>.H<sub>2</sub>SO<sub>4</sub> / NaOH / EtOH / reflux 15 h; (iii) POCl<sub>3</sub> / *N,N*-dimethylaniline / reflux 10 h (iv) Anilines / acetone / reflux 3 h.

**Scheme 2.** Reagents and conditions: (i) THF / Et<sub>3</sub>N / rt 15 h; (ii) H<sub>2</sub> / Pd/C / MeOH / rt 3 h; (iii) Acetone / reflux 2 h.

**Table 1.** VEGFR2 kinase inhibitory activity of the synthesized compounds.

| Compound  | R                                 | IC <sub>50</sub> (μM) | Compound         | R                       | IC <sub>50</sub> (μM) |
|-----------|-----------------------------------|-----------------------|------------------|-------------------------|-----------------------|
| <b>4a</b> | H                                 | 5.76±0.58             | <b>7a</b>        | H                       | 0.473±0.03            |
| <b>4b</b> | 3-CF <sub>3</sub>                 | 3.97±0.43             | <b>7b</b>        | 3-CF <sub>3</sub>       | 0.460±0.05            |
| <b>4c</b> | 4-CN                              | 5.12±0.54             | <b>7c</b>        | 4-CN                    | 0.381±0.04            |
| <b>4d</b> | 2-Cl                              | 3.68±0.40             | <b>7d</b>        | 2-Cl                    | 0.141±0.02            |
| <b>4e</b> | 3-Cl                              | 4.67±0.49             | <b>7e</b>        | 3-Cl                    | 0.118±0.01            |
| <b>4f</b> | 4-Cl                              | 3.87±0.39             | <b>7f</b>        | 4-Cl                    | 0.114±0.01            |
| <b>4g</b> | 3-CF <sub>3</sub> -4-Cl           | 1.34±0.16             | <b>7g</b>        | 3-CF <sub>3</sub> -4-Cl | 0.086±0.01            |
| <b>4h</b> | 3-OCH <sub>3</sub>                | 0.754±0.07            | <b>7h</b>        | 3-OCH <sub>3</sub>      | 0.083±0.01            |
| <b>4i</b> | 4-OCH <sub>3</sub>                | 3.45±0.34             | <b>7i</b>        | 4-OCH <sub>3</sub>      | 0.086±0.01            |
| <b>4j</b> | 4-SO <sub>2</sub> NH <sub>2</sub> | 0.636±0.06            | <b>Sorafenib</b> |                         | 0.090±0.01            |

Data were expressed as Mean ± Standard error (S.E.) of three independent experiments.

**Table 2.** Docking energy scores (*S*) in kcal/mol for compounds **4** and **7**.

| <b>Compound</b> | <b>Energy score<br/>(<i>S</i>) kcal/mol</b> | <b>Compound</b>  | <b>Energy score (<i>S</i>)<br/>kcal/mol</b> |
|-----------------|---|------------------|---|
| <b>4a</b>       | -14.74                                      | <b>7a</b>        | -18.18                                      |
| <b>4b</b>       | -16.09                                      | <b>7b</b>        | -19.27                                      |
| <b>4c</b>       | -15.18                                      | <b>7c</b>        | -18.08                                      |
| <b>4d</b>       | -14.94                                      | <b>7d</b>        | -18.75                                      |
| <b>4e</b>       | -15.11                                      | <b>7e</b>        | -17.85                                      |
| <b>4f</b>       | -15.06                                      | <b>7f</b>        | -18.23                                      |
| <b>4g</b>       | -16.32                                      | <b>7g</b>        | -20.25                                      |
| <b>4h</b>       | -15.51                                      | <b>7h</b>        | -19.12                                      |
| <b>4i</b>       | -15.24                                      | <b>7i</b>        | -19.86                                      |
| <b>4j</b>       | -15.94                                      | <b>Sorafenib</b> | -15.19                                      |

**Table 3.** Percentage growth inhibition (GI %) of *in-vitro* subpanel tumor cell lines at 10  $\mu$ M concentration for seventeen compounds.

| Subpanel                          | Compound <sup>a</sup> |    |    |    |    |    |    |    |    |    |    |    |    |     |    |    |    |
|-----------------------------------|-----------------------|----|----|----|----|----|----|----|----|----|----|----|----|-----|----|----|----|
|                                   | 4a                    | 4b | 4c | 4e | 4f | 4g | 4h | 4i | 7a | 7b | 7c | 7d | 7e | 7f  | 7g | 7h | 7i |
| <b>Leukemia</b>                   |                       |    |    |    |    |    |    |    |    |    |    |    |    |     |    |    |    |
| CCRF-CEM                          | -                     | 39 | -  | -  | 46 | 52 | -  | -  | 34 | 35 | 47 | -  | 41 | 42  | 55 | -  | 40 |
| K-562                             | -                     | 49 | -  | 45 | 48 | 60 | -  | -  | -  | -  | 50 | -  | 30 | -   | 43 | -  | -  |
| MOLT-4                            | -                     | 60 | -  | 37 | 48 | 69 | -  | 31 | 30 | 37 | 56 | -  | -  | 44  | 50 | -  | 47 |
| RPMI-8226                         | 58                    | 87 | -  | 89 | 69 | 94 | 77 | -  | 46 | 42 | 95 | 33 | 31 | 75  | 66 | 43 | 91 |
| SR                                | 30                    | 52 | -  | 43 | 54 | 43 | 35 | 34 | -  | 34 | 43 | -  | -  | 40  | 40 | -  | 39 |
| <b>Non-Small Cell Lung Cancer</b> |                       |    |    |    |    |    |    |    |    |    |    |    |    |     |    |    |    |
| A549/ATCC                         | -                     | 57 | -  | 45 | 40 | 62 | -  | -  | -  | 35 | 36 | -  | 35 | 33  | 48 | -  | -  |
| HOP-62                            | -                     | -  | -  | -  | 40 | -  | 35 | -  | -  | -  | 33 | -  | -  | -   | -  | -  | 33 |
| HOP-92                            | 49                    | 63 | 36 | 63 | 76 | 58 | 53 | 55 | -  | -  | -  | -  | -  | -   | -  | -  | -  |
| NCI-H226                          | -                     | 40 | -  | 35 | 34 | 43 | 37 | -  | -  | -  | -  | -  | -  | -   | -  | -  | -  |
| NCI-H23                           | -                     | 42 | -  | -  | 39 | 40 | -  | -  | -  | -  | -  | -  | -  | -   | -  | -  | -  |
| NCI-H322M                         | -                     | -  | -  | -  | 45 | 37 | -  | -  | -  | -  | -  | -  | -  | -   | 30 | -  | -  |
| NCI-H460                          | -                     | 50 | -  | 34 | 45 | 74 | -  | -  | -  | -  | 40 | -  | -  | 110 | 36 | -  | -  |
| NCI-H522                          | -                     | 45 | -  | 50 | 38 | 49 | 63 | -  | 48 | 56 | 54 | 33 | 57 | 43  | 68 | -  | 36 |
| <b>Colon Cancer</b>               |                       |    |    |    |    |    |    |    |    |    |    |    |    |     |    |    |    |
| COLO 205                          | -                     | -  | -  | -  | -  | -  | -  | -  | -  | -  | -  | -  | -  | -   | 30 | -  | -  |
| HCC-2998                          | -                     | 31 | -  | -  | -  | 42 | -  | -  | -  | -  | -  | -  | -  | -   | -  | -  | -  |
| HCT-116                           | -                     | 56 | -  | 49 | 66 | 73 | 40 | 34 | 35 | 42 | 44 | -  | 37 | 42  | 53 | -  | 34 |
| HCT-15                            | -                     | 41 | -  | 33 | 33 | 58 | -  | -  | -  | -  | 36 | -  | -  | 41  | 40 | -  | 39 |
| HT29                              | -                     | 49 | -  | 31 | 59 | 48 | -  | -  | -  | -  | 45 | -  | -  | 34  | 61 | -  | 34 |
| KM12                              | -                     | 40 | -  | -  | 30 | 52 | -  | -  | -  | 36 | 37 | -  | -  | 39  | 51 | -  | 39 |
| SW-620                            | -                     | -  | -  | -  | -  | -  | -  | -  | -  | -  | -  | -  | -  | -   | -  | -  | -  |
| <b>CNS Cancer</b>                 |                       |    |    |    |    |    |    |    |    |    |    |    |    |     |    |    |    |
| SF-268                            | -                     | -  | -  | -  | -  | -  | -  | -  | -  | -  | -  | -  | -  | -   | -  | -  | -  |
| SF-295                            | -                     | 38 | -  | 33 | 50 | 49 | -  | 30 | -  | -  | 86 | -  | -  | 52  | 50 | -  | 81 |
| SF-539                            | -                     | 36 | -  | 35 | 46 | 42 | -  | -  | -  | -  | 67 | -  | -  | 41  | -  | 35 | 49 |
| SNB-19                            | -                     | 45 | -  | 37 | 38 | 45 | 30 | -  | -  | 30 | 43 | -  | -  | 39  | 45 | -  | -  |
| SNB-75                            | -                     | -  | -  | 32 | -  | -  | 41 | -  | -  | 31 | 57 | -  | -  | 49  | 59 | -  | 50 |
| U251                              | -                     | 44 | -  | 34 | 38 | 59 | -  | -  | 32 | 30 | 63 | -  | -  | 48  | 51 | 32 | 49 |
| <b>Melanoma</b>                   |                       |    |    |    |    |    |    |    |    |    |    |    |    |     |    |    |    |
| LOX IMVI                          | -                     | -  | -  | -  | 58 | -  | -  | -  | -  | -  | 46 | -  | -  | -   | 32 | -  | -  |
| MALME-3M                          | -                     | -  | -  | -  | -  | -  | -  | -  | -  | -  | 42 | -  | -  | -   | -  | -  | 31 |
| M14                               | -                     | -  | -  | -  | 47 | 48 | -  | -  | -  | 30 | 35 | -  | -  | 30  | 40 | -  | -  |
| MDA-MB-435                        | -                     | -  | -  | -  | 30 | -  | -  | -  | -  | -  | -  | -  | -  | -   | 35 | -  | -  |
| SK-MEL-28                         | -                     | -  | -  | -  | -  | -  | -  | -  | -  | -  | -  | -  | -  | -   | -  | -  | -  |
| SK-MEL-5                          | -                     | -  | -  | -  | -  | -  | -  | -  | -  | -  | 45 | -  | -  | -   | -  | -  | -  |
| UACC-257                          | -                     | -  | -  | -  | 35 | -  | -  | -  | -  | -  | 33 | -  | -  | -   | 36 | -  | -  |
| UACC-62                           | -                     | -  | -  | -  | -  | -  | -  | -  | -  | -  | -  | -  | -  | -   | -  | -  | -  |
| -                                 | -                     | 42 | -  | 39 | 60 | 41 | -  | 34 | -  | -  | -  | -  | -  | -   | -  | -  | -  |
| <b>Ovarian Cancer</b>             |                       |    |    |    |    |    |    |    |    |    |    |    |    |     |    |    |    |
| IGROV1                            | -                     | 37 | -  | -  | 36 | 32 | 33 | -  | -  | -  | 46 | -  | -  | -   | 53 | -  | -  |
| OVCAR-3                           | -                     | 48 | -  | 34 | 40 | 59 | -  | -  | -  | -  | -  | -  | -  | -   | 78 | -  | -  |
| OVCAR-4                           | -                     | 37 | -  | -  | 33 | 45 | -  | -  | -  | -  | -  | -  | -  | -   | 60 | -  | -  |
| OVCAR-5                           | -                     | -  | -  | -  | -  | 33 | -  | -  | -  | -  | -  | -  | -  | -   | 30 | -  | -  |
| OVCAR-8                           | -                     | 35 | -  | -  | 35 | 40 | -  | -  | -  | -  | -  | -  | -  | -   | 66 | -  | -  |
| NCI/ADR-RES                       | -                     | 40 | -  | 32 | 48 | 50 | 30 | -  | -  | -  | -  | -  | -  | -   | 67 | -  | -  |
| SK-OV-3                           | -                     | -  | -  | -  | -  | -  | -  | -  | -  | -  | 37 | -  | -  | -   | 38 | -  | -  |
| <b>Renal Cancer</b>               |                       |    |    |    |    |    |    |    |    |    |    |    |    |     |    |    |    |
| 786-0                             | -                     | 33 | -  | -  | 43 | 41 | -  | -  | 36 | 41 | 83 | 41 | 35 | 58  | 62 | 42 | 63 |
| A498                              | 35                    | 40 | 30 | 34 | 53 | 46 | -  | 47 | -  | -  | 54 | 44 | -  | 32  | -  | -  | -  |
| ACHN                              | -                     | 31 | -  | 31 | 47 | 45 | -  | -  | -  | 41 | 48 | -  | 39 | 46  | 50 | -  | 32 |

|  |           |           |           |           |           |           |           |           |           |           |           |           |           |           |           |           |           |
|--|-----------|-----------|-----------|-----------|-----------|-----------|-----------|-----------|-----------|-----------|-----------|-----------|-----------|-----------|-----------|-----------|-----------|
| CAKI-1                                 | -         | 32        | -         | -         | 37        | 35        | -         | -         | -         | -         | -         | -         | -         | -         | -         | -         | -         |
| RXF 393                                | -         | 34        | -         | -         | 32        | 33        | 32        | -         | 49        | 50        | 110       | 48        | 40        | 79        | 72        | 50        | 100       |
| SN12C                                  | -         | 46        | -         | 34        | 50        | 46        | -         | 34        | -         | -         | -         | -         | -         | -         | -         | -         | -         |
| TK-10                                  | -         | -         | -         | -         | 52        | 40        | -         | -         | -         | -         | -         | -         | -         | -         | -         | -         | -         |
| UO-31                                  | 38        | 66        | 49        | 61        | 68        | 63        | 57        | 43        | -         | -         | 44        | -         | -         | -         | -         | -         | -         |
| <b>Prostate Cancer</b>                 |           |           |           |           |           |           |           |           |           |           |           |           |           |           |           |           |           |
| PC-3                                   | -         | 49        | 34        | 42        | 51        | 61        | 30        | -         | 30        | 36        | 41        | -         | 32        | 31        | 45        | -         | 30        |
| DU-145                                 | -         | -         | -         | -         | 42        | 37        | -         | -         | -         | -         | -         | -         | -         | -         | -         | -         | -         |
| <b>Breast Cancer</b>                   |           |           |           |           |           |           |           |           |           |           |           |           |           |           |           |           |           |
| MCF7                                   | -         | 35        | -         | -         | 36        | 48        | -         | 38        | -         | -         | 45        | 32        | -         | 33        | 46        | -         | 30        |
| HS 578T                                | -         | -         | -         | -         | 35        | 34        | -         | -         | 33        | 34        | 105       | -         | -         | 75        | 48        | 50        | 96        |
| BT-549                                 | -         | -         | -         | -         | -         | -         | -         | -         | -         | -         | 51        | -         | -         | 37        | -         | -         | 31        |
| T-47D                                  | -         | 56        | 50        | 41        | 44        | 59        | 30        | 46        | 41        | -         | 48        | 52        | 39        | 37        | 47        | -         | 42        |
| MDA-MB-468                             | -         | 42        | 30        | 30        | 42        | 54        | -         | -         | -         | -         | -         | -         | -         | 37        | -         | -         | -         |
| MDA-MB-231/ATCC                        | -         | 46        | -         | 39        | 36        | 40        | 37        | 36        | 31        | -         | 63        | -         | -         | 30        | 41        | -         | 46        |
| <b><u>Mean inhibition, %</u></b>       | <b>22</b> | <b>37</b> | <b>15</b> | <b>29</b> | <b>40</b> | <b>44</b> | <b>22</b> | <b>21</b> | <b>17</b> | <b>21</b> | <b>39</b> | <b>15</b> | <b>18</b> | <b>32</b> | <b>33</b> | <b>12</b> | <b>30</b> |
| <b><u>Sensitive cell lines no.</u></b> | <b>5</b>  | <b>39</b> | <b>6</b>  | <b>29</b> | <b>46</b> | <b>44</b> | <b>16</b> | <b>12</b> | <b>12</b> | <b>17</b> | <b>36</b> | <b>7</b>  | <b>11</b> | <b>27</b> | <b>38</b> | <b>6</b>  | <b>24</b> |

<sup>a</sup> Only GI % higher than 30% are shown

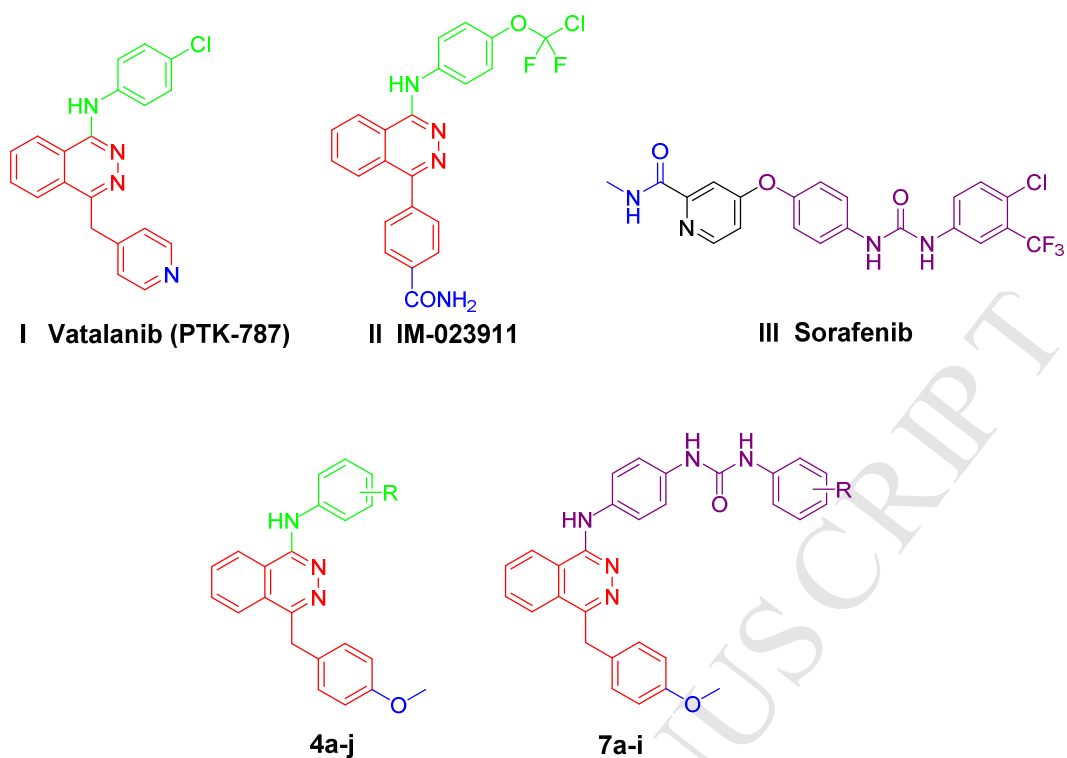


**Figure 1.** Structures of VEGFR-2 inhibitors (I-III) and the target phthalazines 4a-j and 7a-i.

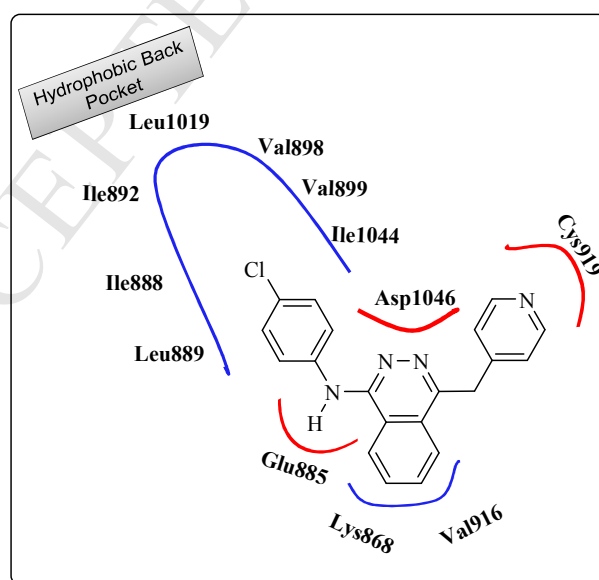


**Figure 2.** 2D schematic diagram representing vatalanib plausible binding mode in the VEGFR-2 active site.

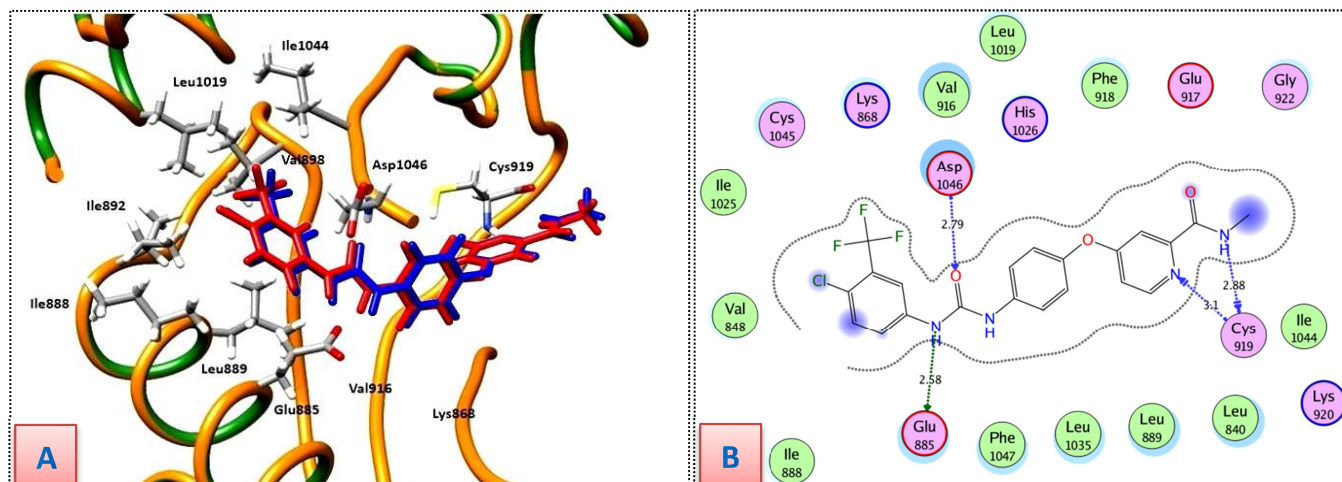


**Figure 3.** (A) Superimposition of the co-crystallized (blue) and the docking pose (red) of sorafenib in the VEGFR-2 active site with RMSD of 0.470Å. (B) 2D interaction diagram showing sorafenib docking pose interactions with the key amino acids in the VEGFR-2 active site. (Distances in Å)

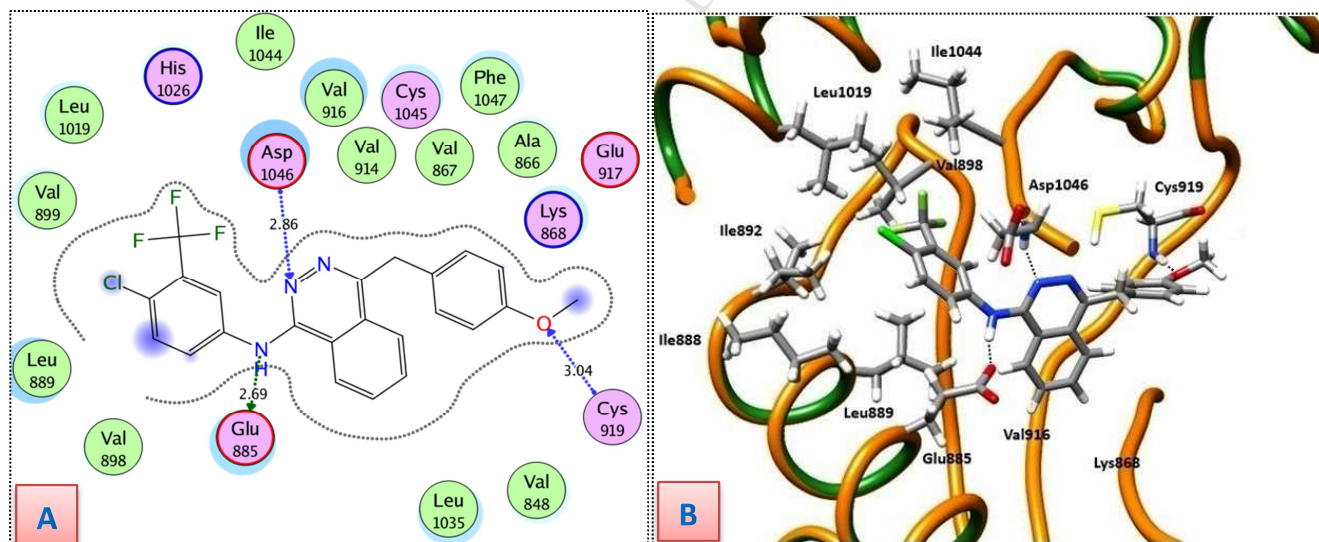


**Figure 4.** 2D diagram (A) and 3D representation (B) of compound **4g** showing its interaction with the VEGFR-2 receptor active site.

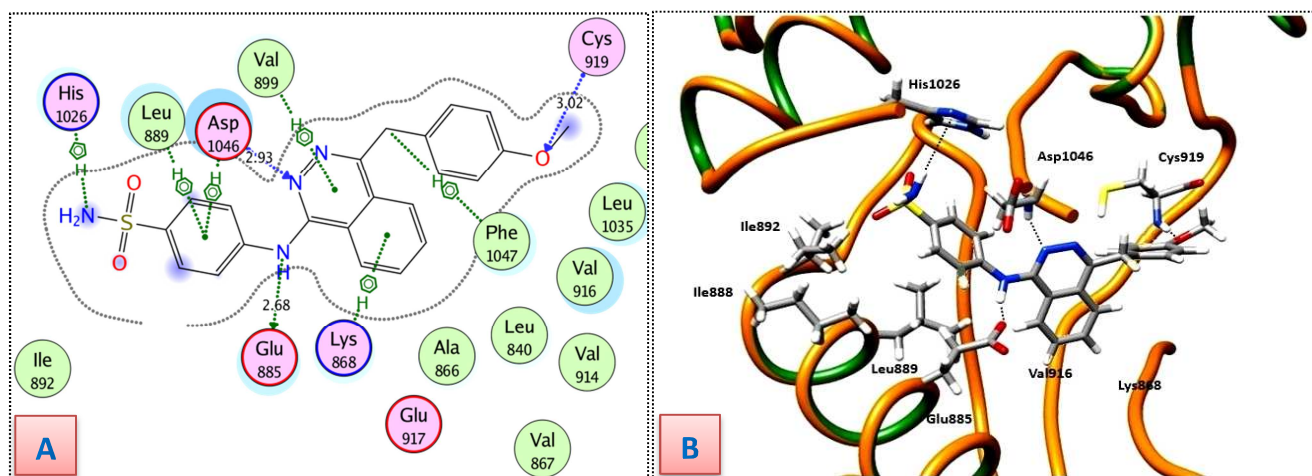


**Figure 5.** 2D diagram (A) and 3D representation (B) for compound **4j** showing its interaction with the VEGFR-2 receptor active site.

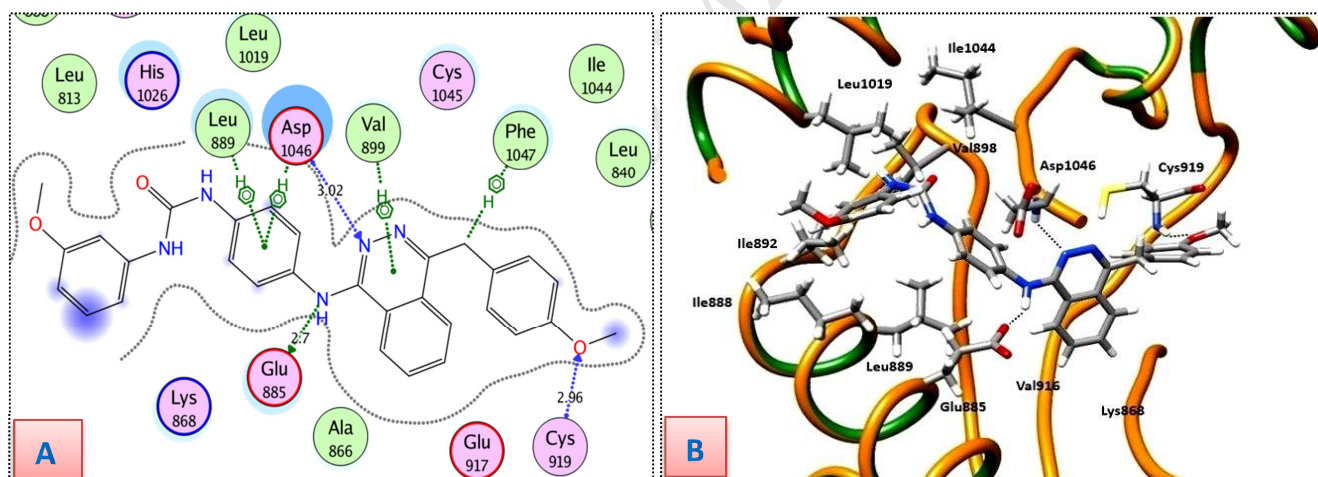


**Figure 6.** 2D diagram (A) and 3D representation (B) for compound **7h** showing its interaction with the VEGFR-2 receptor active site.

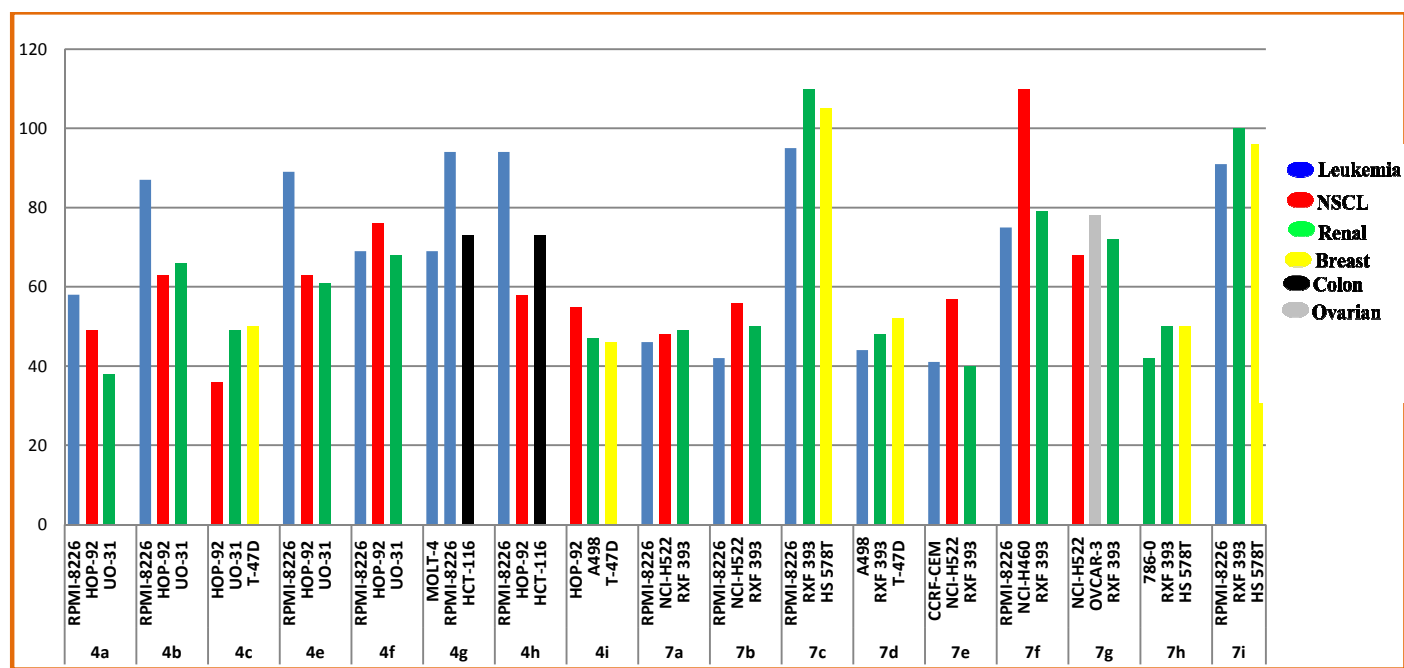
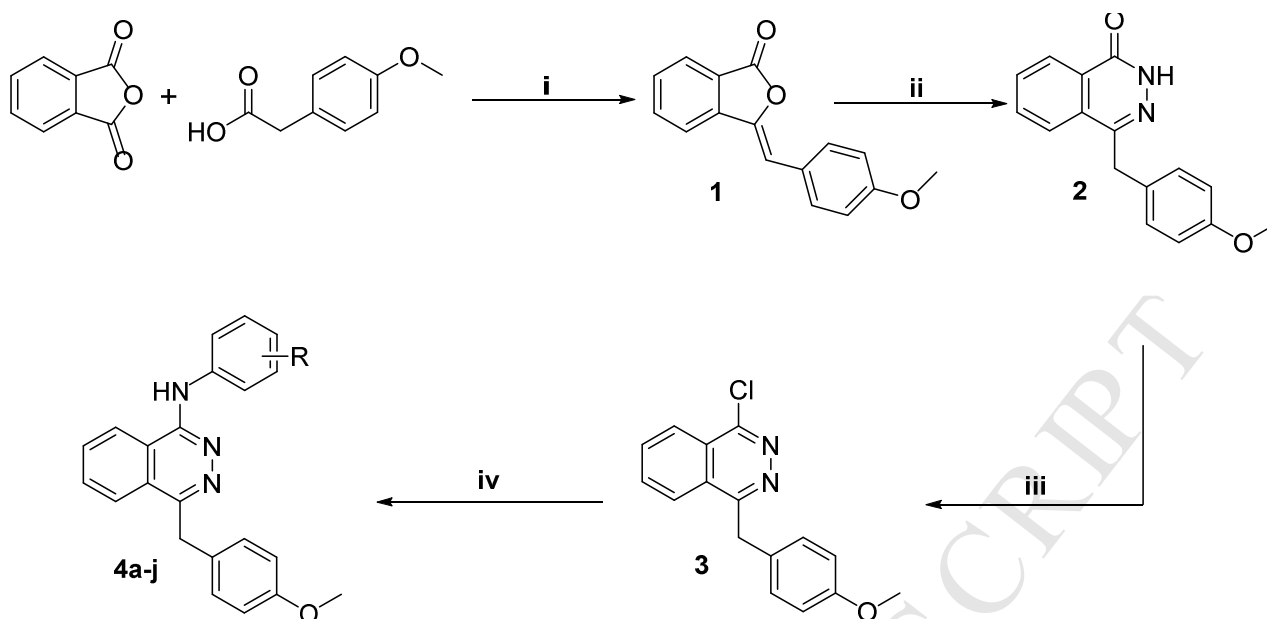
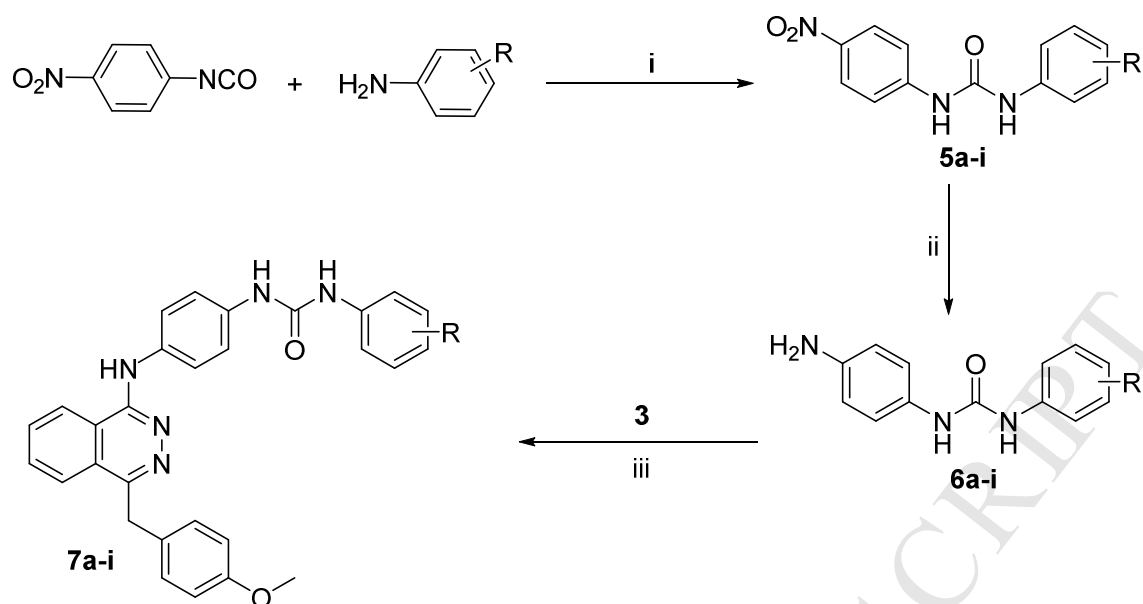


**Figure 7.** The most sensitive cell lines towards the target compounds **4a-j** and **7a-i** according to the GI %.



R, **a** = H; **b** = 3-CF<sub>3</sub>; **c** = 4-CN; **d** = 2-Cl; **e** = 3-Cl; **f** = 4-Cl; **g** = 4-Cl-3-CF<sub>3</sub>; **h** = 3-OCH<sub>3</sub>;  
**i** = 4-OCH<sub>3</sub>; **j** = 4-SO<sub>2</sub>NH<sub>2</sub>

**Scheme 1.** Reagents and conditions: **(i)** CH<sub>3</sub>COONa / heating 200 °C 5 h; **(ii)** NH<sub>2</sub>NH<sub>2</sub>·H<sub>2</sub>SO<sub>4</sub>/ NaOH/EtOH / reflux 15 h; **(iii)** POCl<sub>3</sub> / *N,N*-dimethylaniline / reflux 10 h **(iv)** Anilines / acetone / reflux 3 h.



R, **a** = H; **b** = 3-CF<sub>3</sub>; **c** = 4-CN; **d** = 2-Cl; **e** = 3-Cl; **f** = 4-Cl; **g** = 4-Cl-3-CF<sub>3</sub>; **h** = 3-OCH<sub>3</sub>; **i** = 4-OCH<sub>3</sub>

**Scheme 2.** Reagents and conditions: (i) THF / Et<sub>3</sub>N / rt 15 h; (ii) H<sub>2</sub> / Pd/C / MeOH / rt 3 h; (iii) Acetone / reflux 2 h.

## Highlights

- Two series of 4-(4-Methoxybenzyl)phthalazines **4a-j** & **7a-i** were synthesized.
- The prepared phthalazines were evaluated for their inhibitory activity against VEGFR-2.
- Molecular docking was used to improve the binding affinity for **4a-j** towards VEGFR-2.
- **7g-i** inhibited VEGFR-2 with  $IC_{50} = 0.086, 0.083$  and  $0.086 \mu\text{M}$ .
- Anticancer activity of the synthesized compounds was screened by the (NCI), USA.